

# Asteroids *Do* Have Satellites

**William J. Merline**

*Southwest Research Institute (Boulder)*

**Stuart J. Weidenschilling**

*Planetary Science Institute*

**Daniel D. Durda**

*Southwest Research Institute (Boulder)*

**Jean-Luc Margot**

*California Institute of Technology*

**Petr Pravec**

*Astronomical Institute AS CR, Ondřejov, Czech Republic*

**and**

**Alex D. Storrs**

*Towson University*

After years of speculation, satellites of asteroids have now been shown definitively to exist. Asteroid satellites are important in at least two ways: (1) they are a natural laboratory in which to study collisions, a ubiquitous and critically important process in the formation and evolution of the asteroids and in shaping much of the solar system, and (2) their presence allows us to determine the density of the primary asteroid, something which otherwise (except for certain large asteroids that may have measurable gravitational influence on, e.g., Mars) would require a spacecraft flyby, orbital mission, or sample return. Satellites or binaries have now been detected in a variety of dynamical populations, including near-Earth, Main Belt, outer Main-Belt, Trojan, and trans-Neptunian. Detection of these new systems has been the result of improved observational techniques, including adaptive optics on large telescopes, radar, direct imaging, advanced lightcurve analysis, and spacecraft imaging. Systematics and differences among the observed systems give clues to the formation mechanisms. We describe several processes that may result in binary systems, all of which involve collisions of one type or another, either physical or gravitational. Several mechanisms will likely be required to explain the observations.

# 1 INTRODUCTION

## 1.1 Overview

Discovery and study of small satellites of asteroids or double asteroids can yield valuable information about the intrinsic properties of asteroids themselves and about their history and evolution. Determination of the orbits of these moons can provide precise determination of the total (primary + secondary) mass of the system. In the case of a small secondary, the total mass is dominated by the primary. For a binary with determinable size-ratio of components (e.g. double asteroids), an assumption of similar densities can yield the individual masses. If the actual sizes of the primary or the pair are also known, then reliable estimates of the primary's bulk density, a fundamental property, can be made. This reveals much about the composition and structure of the primary and will allow us to make comparisons between, for example, asteroid taxonomic types and our inventory of meteorites. In general, uncertainties in the asteroid size will dominate the uncertainty in density.

Similarities and differences among the detected systems are revealing important clues about the possible formation mechanisms. Systematics are already being seen among the main-belt binaries — many of them are C-like and several are also family members. There are several theories seeking to explain the origin of these binary systems, all of them involving disruption of the parent object, either by physical collisions, or gravitationally during a close pass to a planet. It is likely that several of the mechanisms will be required to explain the observations.

The presence of a satellite provides a real-life laboratory to study the outcome of collisions and gravitational interactions. The current population probably reflects a steady state process of creation and destruction. The nature and prevalence of these systems will therefore help us understand the collisional environment in which they formed, and have further implications for the role of collisions in shaping our solar system. They will also provide clues to the dynamical history and evolution of the asteroids.

A decade ago, binary asteroids were mostly a theoretical curiosity, despite sporadic unconfirmed satellite detections. In 1993, the *Galileo* spacecraft made the first undeniable detection of an asteroid moon, with the discovery of Dactyl, a small moon of Ida. Since that time, and particularly in the last year, the number of known binaries has risen dramatically. In the mid-late 1990s, the tell-tale lightcurves of several near-Earth asteroids (NEAs) revealed a high likelihood of being double. Previously odd-shaped and lobate near-Earth asteroids, observed by radar, have given way to signatures revealing that at least five NEAs are binary systems. Indications from these lightcurve and radar observations are that among the NEAs, the binary frequency may be about 16% (see Sections 2.4 & 2.5).

Among the main-belt asteroids, we now know of 8 confirmed binary systems, although their overall frequency is likely to be low, perhaps a few percent (see Section 2.2.6). These detections have largely come about because of significant advances in adaptive optics systems on large telescopes, which can now reduce the blurring of the Earth's atmosphere to compete with the spatial resolution of space-based imaging (which itself, via HST, is now contributing valuable observations). Searches among the Trojans and Trans-Neptunian Objects (TNOs) have shown that other dynamical populations also harbor binaries.

Now that we have reliable techniques for detection, we have been rewarded with many examples of systems for study. This has in turn spurred new theoretical thinking and numerical

simulations, the techniques for which have also improved substantially in recent years.

## 1.2 History and Inventory of Binary Asteroids

Searches for satellites can be traced back to William Herschel in 1802, soon after the discovery of the first asteroid, (1) Ceres. The first suspicion of a satellite goes back to Andre (1901), who speculated that the  $\beta$ -Lyrae-like lightcurve of Eros could result from an eclipsing binary system. Of course, we now know definitively that this interpretation is wrong (Merline *et al.* 2001c), Eros being one of the few asteroids visited directly by a spacecraft (*cf.* Cheng, this volume).

In the late 1970s, there was a flurry of reports of asteroid satellites, inferred from indirect evidence, such as anomalous lightcurves or spurious secondary blink-outs during occultations of stars by asteroids. Van Flandern *et al.* (1979) in *Asteroids I* gives a complete summary of the evidence as of that time. To some, the evidence was highly suggestive that satellites were common. To date, however, none of those suspected binaries has been shown to be real, despite rather intensive study with modern techniques.

In the 1980s, additional lines of evidence were pursued, including asteroids with slow rotation, or fast rotation, and the existence of doublet craters on, *e.g.*, the Moon or Earth. Cellino *et al.* (1985) studied 10 asteroids that showed anomalous lightcurves, which they compared with predictions from models of equilibrium binaries of varying mass ratios by Leone *et al.* (1984). Model separations and magnitude differences for these putative binaries were given; most of these could have been detected using by modern observations, but none have been confirmed as separated binaries (although Ostro *et al.* (2000a), Merline *et al.* (2000b), and Tanga *et al.* (2001) have shown (216) Kleopatra to be a contact binary). In the same decade, radar emerged as a technique capable of studying a small number of (generally nearby) asteroids. In addition, speckle interferometry was used to search for close-in binaries, and the advent of CCD technology allowed more sensitive and detailed searches. Studies by Gehrels, Drummond, & Levenson (1987), who searched 11 main-belt asteroids using direct CCD-imaging and by Gradie & Flynn (1988), who searched 17 main-belt asteroids, using a CCD/coronagraphic technique, did not produce any detections. By the end of the decade, the previous optimism about the prevalence of satellites had retreated to claims ranging from them being essentially nonexistent (Gehrels, Drummond, & Levenson 1987) to being rare (Weidenschilling *et al.* 1989). Weidenschilling *et al.* (1989) gives a summary of the status of the observations and theory as of the time of *Asteroids II*.

The tide turned, however, in 1993, when the *Galileo* spacecraft, en route to its orbital tour of the Jupiter system, flew past (243) Ida, and serendipitously imaged a small (1.4-km diameter Dactyl) moon orbiting this 31-km diameter, S-type asteroid. This discovery spurred new observations and theoretical thinking on the formation and prevalence of asteroid satellites. Roberts, McAlister, & Hartkopf (1995) performed a search of 57 asteroids, in multiple observing sessions, using speckle interferometry. No companions were found in this survey. A search by Storrs *et al.* (1999a) of 10 asteroids using HST also revealed no binaries. Numerical simulations performed by Durda (1996) and Doressoundiram *et al.* (1997) showed that the formation of small satellites may be a fairly common outcome of catastrophic collisions. Bottke & Melosh (1996a,b) suggested that a sizeable fraction ( $\sim 15\%$ ) of Earth-crossing asteroids may have satellites, based on their simulations and the occurrence of doublet craters on the Earth and Venus. Various theoretical studies were performed of the dynamics and stability of orbits about irregularly-shaped asteroids (Chauvineau & Mignard 1990; Hamilton & Burns 1991; Chauvineau, Farinella, & Mignard 1993; Scheeres

1994).

After the first imaging of an asteroid moon by *Galileo*, several reports of binaries among the near-Earth asteroid population, based on lightcurve shapes, were made by Pravec *et al.* and Mottola *et al.*, including 1994 AW<sub>1</sub> (Pravec & Hahn 1997), 1991 VH (Pravec, Wolf, & Šarounová 1998), 3671 Dionysus (Mottola *et al.* 1997, *IAUC* **6680**), and 1996 FG<sub>3</sub> (Pravec, Šarounová, & Wolf 1998, *IAUC* **7074**). While these systems are likely to be real, they have not been confirmed by direct imaging or radar techniques.

It was not until 1998 that the first definitive and verifiable evidence for an asteroid satellite was acquired from Earth, when 215-km (45) Eugenia was found to have a small moon (13-km Petit Prince) by direct imaging assisted by adaptive optics (AO) (Merline *et al.* 1999b,c). This discovery was the first result from a dedicated survey with the capability to search for faint companions ( $\Delta m \sim 7$  mag) as close as a few tenths of an arcsecond from the primary. This survey detected two more asteroid binaries in 2000 — (762) Pulcova (Merline *et al.* 2000a) and (90) Antiope (Merline *et al.* 2000a, 2000b). While the moon of Pulcova is small, Antiope is truly a double asteroid, with components of nearly the same size.

After these detections, the first two near-Earth asteroid binaries to be definitively detected by radar were announced: 2000 DP<sub>107</sub> (Ostro *et al.* 2000b, *IAUC* **7496**; Margot *et al.* 2000, *IAUC* bf 7503) and 2000 UG<sub>11</sub> (Nolan *et al.* 2000, *IAUC* **7518**). In the meantime and since, Pravec *et al.* continued to add to the rapidly growing list of suspected binary NEAs from lightcurves.

Starting in 2001, binary discoveries really surged. In February, Brown & Margot (2001, *IAUC* **7588**), also using adaptive optics technology, discovered a moon of (87) Sylvia, a Cybele asteroid beyond the Main Belt. Soon afterwards, Storrs *et al.* (2001, *IAUC* **7599**) reported a moon of (107) Camilla, also a Cybele, using Hubble Space Telescope. Three additional radar binaries were announced — 1999 KW<sub>4</sub> (Benner *et al.* 2001a, *IAUC* **7632**) and 1998 ST<sub>27</sub> (Benner *et al.* 2001b, *IAUC* **7730**) and 2002 BM<sub>26</sub> (Nolan *et al.* 2002, *IAUC* **7824**). In addition, Veillet *et al.* (2002; 2001, *IAUC* **7610**) reported the first binary among Trans-Neptunian Objects (aside from Pluto/Charon), 1998 WW<sub>31</sub>, obtained by direct CCD imaging without AO. Six more TNO doubles were reported: 2001 QT<sub>297</sub>, Eliot *et al.* (2001, *IAUC* **7733**); 2001 QW<sub>322</sub>, Kavelaars *et al.* (2001, *IAUC* **7749**); 1999 TC<sub>36</sub>, Trujillo & Brown (2002, *IAUC* **7787**); 1998 SM<sub>165</sub>, Brown & Trujillo (2002, *IAUC* **7807**); 1997 CQ<sub>29</sub>, Noll *et al.* (2002a, *IAUC* **7824**); and 2000 CF<sub>105</sub>, Noll *et al.* (2002b, *IAUC* **7857**). A small moon was co-discovered around (22) Kalliope by Margot & Brown (2001), *IAUC* **7703** and Merline *et al.* (2001a, *IAUC* **7703**), which is the first M-type asteroid known to have a companion. Later, the first binary Trojan asteroid, (617) Patroclus, was found (Merline *et al.* 2001b, *IAUC* **7741**); this asteroid, like Antiope, has components of nearly equal size. Merline *et al.* (2002, *IAUC* **7827**) then detected a widely-spaced binary in the Main Belt, (3749) Balam, which appears to be the most loosely-bound system known. (The list of asteroid satellites in this chapter is complete through 2002 May).

### 1.3 Observational Challenges

Direct imaging of possible satellites of asteroids has been hampered by lack of adequate angular resolution to distinguish objects separated by fractions of an arcsecond and by lack of sufficient dynamic range of detectors to resolve differences in brightness of many magnitudes. The basic observational problem, detection of a faint object in the presence of a much brighter one, is common to many areas of astronomy, such as binary and multiple star systems or circumstellar and

proto-stellar disks.

At the inner limit, the smallest separations between the primary asteroid and the companion are determined by orbital instabilities (a few radii of the primary), and at the far extreme by the Hill stability limit (a few hundred radii of the primary for the Main Belt). For a 50 km diameter main-belt asteroid (say at 2.5 AU), observed at opposition, the angular separation at which we might find a satellite spans the range of about 0.05 arcsec to several arcsec. If the satellite has a diameter of 2 km, the brightness difference is 7 magnitudes. Using conventional telescopes, the overlapping point spread functions of these objects, of widely-disparate brightness, make satellite detection in the near field extraordinarily challenging. The FWHM of the uncorrected point spread function of a large ground-based telescope, under average seeing conditions of 1 arcsec, corresponds to nearly 25 primary radii in the above example. Indeed, both theory and most examples of observed binaries suggest that moons are more likely to be found closer to the primary.

The traditional techniques have been deep imaging using multiple short exposures to search the near field and the use of “coronagraphic” cameras for the far field. With modern, low-noise, high-dynamic-range detectors and with the advent of adaptive optics technology, a ground-based search for and study of, asteroid satellites has been realized.

Radar is a powerful technique for nearby objects because the return signal is proportional to the inverse 4th power of the distance. This has limited study to either very large asteroids at the inner edge of the Main Belt or to NEAs. Radar has shown tremendous promise and upgrades to the telescopes and electronics are enhancing the range and capabilities. Observations of NEAs, however, have drawbacks because the objects are small and opportunities to observe them may be spaced many years apart. Therefore, it is difficult to make repeat or different observations.

Lightcurve observations generally require the observed system to be non-synchronous, *i.e.*, having the primary’s rotation rate be different than the orbital rate. In addition, either the system must be eclipsing or the secondary must have an elongated shape. Such a system will show a two-component lightcurve. To be well resolved, both contributions should have an amplitude of at least a few hundredths of a magnitude. The requirements generally restrict efficient observations to close-in binary systems with the secondary’s diameter at least  $\sim \frac{1}{5}$  that of the primary. This technique works best also on NEAs, where these small binaries appear to have a long tidal evolution timescale and therefore can remain non-synchronous for a long time after formation. These close binaries also lend themselves to having a high probability of eclipse at any given time. This technique suffers from the same problems with NEAs mentioned above — repeat observations over a wide range of viewing geometries are not possible quickly. Thus, in many cases there may be ambiguities in interpretation of the lightcurve signatures.

Direct imaging has been shown to be possible for TNOs because of those detected so far have wide separations and large secondary/primary size ratios. So although these objects are far away ( $\sim 45$  AU), loosely-bound binaries can be separated with conventional (non-AO) imaging under ideal conditions. HST searches for main-belt binaries have largely been unsuccessful, not because of limitations to the instrumentation, but because of the lack of telescope time allocated. HST searches for TNO binaries are now underway and are showing promising results.

## 2 OBSERVATIONAL TECHNIQUES AND DISCOVERIES

### 2.1 Searches during Spacecraft Encounters

One of the most effective ways of performing a search for satellites of asteroids is by a flyby or orbital tour with a spacecraft, although this is prohibitively expensive for more than a few objects. Nonetheless, this method produced the first definitive evidence that asteroid moons can exist and also allows searches to much smaller sizes than is possible from Earth.

There are a variety of problems encountered when searching for satellites from images taken during spacecraft encounters. A major one is that the images are taken from a rapidly moving platform. This makes quick visual inspection difficult, because one must project the image to a common reference point. If the moon is resolved, as in the case of Dactyl, the problem is more manageable. But it is possible that moons would be small, appearing as point-like objects, and would compete for recognition with stars, cosmic ray hits, and detector defects. The strategy is normally to take a series of many pictures, in which the detector defects are known and the cosmic rays may be eliminated by lack of persistence. Stars may be eliminated by identification using star catalogs, or by common motion. Even with these techniques, however, cosmic ray hits in a series of images may conspire to cluster in a pattern that is consistent with the spacecraft motion and an object in a plausible position in 3-D space relative to the asteroid. Correlations among all identified point-source candidates on a series of images must be examined.

#### 2.1.1 Discovery of Dactyl

The first image of an asteroid moon was spotted by Ann Harch of the *Galileo* Imaging Team on February 17, 1994, during the playback of images from *Galileo*'s encounter with S-type 243 Ida on August 29, 1993. Because of the loss, early in the mission, of *Galileo*'s high gain antenna, some data from the Ida encounter was returned months afterwards. The first images were returned as "jailbars", thin strips of a few lines of data separated by gaps. This technique allowed a quick look of the contents of the images, to determine which lines contained Ida data. Fortunately, one of these lines passed through the satellite, as shown in Figure 1. The presence of the moon was later confirmed by the infrared spectrometer experiment and was announced by Belton & Carlson (1994, *IAUC 5948*). It was initially dubbed 1993(243)1, the first satellite of asteroid (243) to be discovered in 1993, and later given the permanent name Dactyl, after the Dactyli, who were either children or protectors of Ida.

During the flyby of Ida, 47 images of Dactyl were obtained (Chapman *et al.* 1995; Belton *et al.* 1995; Belton *et al.* 1996). However, because there was no opportunity for feedback to guide an imaging sequence, these pictures were all serendipitous. The spacecraft trajectory was nearly in the plane of the satellite motion, and hence little relative motion was observed, resulting in poorly determined orbital parameters. Follow-up observations with HST (Belton *et al.* 1995; Belton *et al.* 1996) failed to find the satellite, which was not surprising given its separation. But if the object were on a hyperbolic or highly elliptical orbit, there was some chance of finding it with HST. These additional observations did allow limits to be set on the density of Ida.

Additionally, resolved pictures of Dactyl's surface have given us the opportunity for geological interpretation, and a glimpse into the possible origin and history of an asteroid moon. The pair is shown in Fig. 2, with a smaller-scale image of Dactyl in Fig. 3. Chapman *et al.* 1996 and

Veverka *et al.* 1996b indicate that the crater size-frequency distribution on both Ida and Dactyl exhibit equilibrium-saturation (see also Chapman, this volume). Thus, we can estimate only the minimum ages for both objects; the relative ages of the two, from crater data alone, is uncertain. Given the observed impactor size-distribution, saturation at the largest craters on Ida, of size about 10 km would be expected after about 2 Gyr (Chapman *et al.* 1996), setting roughly the minimum age of Ida. The largest craters on Dactyl, however, are less than 0.4 km in size, and would saturate in about 30 Myr. Impacts that would create larger craters on Dactyl would instead break up the object. The mean time between impacts that would destroy Dactyl was estimated by Davis *et al.* (1996) to be, depending on model assumptions, between about 3 Myr and 240 Myr, the same order as the saturation cratering age. If Dactyl was formed 2 Gyr ago with Ida, via disruptive capture (Section 3.3), perhaps during the Koronis-family breakup (Binzel 1988), then it is very unlikely that it would still exist intact, given its short lifetime against collisional breakup. Conceivably, it may have formed from the ejecta of a more recent, large cratering event (Section 3.2). Either way, it must have been disrupted and reaccreted several times since its initial formation, because it is unlikely to have formed only in the last 30 Myr. Additional geological data supports the idea of this satellite as a reaccumulated rubble pile. It is roughly spherical, with no obvious evidence of coherent monolithic structure. It displays a softened appearance, and likely has a surface regolith (Veverka *et al.* 1996b).

The spectrum of Dactyl (from *Galileo* imager data, 0.4–1.0  $\mu\text{m}$ ) is similar to that of Ida (Veverka *et al.* 1996a), but with some important differences. Both objects show S-type spectra and have similar albedos. Dactyl, however, shows somewhat less reddening than Ida, possibly indicating less space weathering, which is also consistent with a younger surface age, as expected from the most recent disruption/reaccretion episode (Chapman 1996).

### 2.1.2 Other Searches

Extensive searches were made for additional satellites of Ida in the *Galileo* data sets and no candidates were found that were not consistent with single or multiple cosmic ray events (Belton *et al.* 1995; Belton *et al.* 1996). The searches were made at spacecraft-to-asteroid ranges of 200 000 km (satellite-detection size limit  $\sim$  800 m), of 10 000 km (size limit  $\sim$  50 m), and of 2400 km (encounter) with size limit  $\sim$  10 m diameter.

Cursory searches for satellites were made during the *Galileo* flyby of S-type (951) Gaspra in 1991, with no detections of objects larger than 27 m out to about 10 Gaspra radii (Belton *et al.* 1992).

The *NEAR* spacecraft made a fast flyby of C-type, inner main-belt asteroid (253) Mathilde in 1997 en route to its orbital encounter with (433) Eros. A well-planned imaging sequence to search for satellites was performed and a thorough search made (Merline *et al.* 1998; Veverka *et al.* 1999a). Over 200 images were taken specifically to search for satellites. No unambiguous evidence for satellites larger than 40 m diameter was found within the searchable volume, which was estimated to be about 4% of the Hill sphere. The portion, however, of the Hill sphere searched was an important one, inside roughly 20 radii of Mathilde (almost all of the known main-belt binaries show separations well below 20 primary radii). From approach images, which were less sensitive due to lighting geometry, no satellites larger than 10 km were found in the entire Hill sphere.

The *NEAR* spacecraft continued on to an unplanned flyby of (433) Eros, an S-type near-Earth

asteroid, in December 1998 (*cf.* Cheng, this volume). The first critical burn of the main rocket for the rendezvous aborted prematurely, which led to execution of a contingency imaging sequence. This included a search for satellites down to size about 50 m in the entire Hill sphere (Merline *et al.* 1999a; Veverka *et al.* 1999b). About one year later, after engineers had diagnosed the problems and brought the spacecraft slowly back to Eros, the orbital tour of Eros began. During approach to orbit insertion, another, more detailed and thorough search for satellites was made. Here, both manual and automated searches were performed (Merline *et al.* 2001c, Veverka *et al.* 2000). This was the first systematic search for satellites of the entire Hill sphere of an asteroid down to small sizes. The search found no objects at a diameter 20 m (95% confidence), and at 10 m (with 70% confidence).

## 2.2 Adaptive Optics on Large Ground-Based Telescopes

Given the observational challenges just discussed and the number of failed attempts to detect asteroid satellites, it was clear that a new approach was needed. In 1996, Merline and collaborators began to apply a relatively new technology in hopes of achieving high contrast, high spatial resolution imaging on a large number of targets, from ground-based telescopes. This new technique, called adaptive optics (AO), ultimately led to the first Earth-based images of satellites.

### 2.2.1 Method and Capabilities

This technique minimizes the distortion in an astronomical image by sensing and correcting, in real-time, aberrations due to the Earth's atmosphere, usually by means of a deformable mirror. This new technology can result in diffraction-limited imaging with the largest ground-based telescopes. Compared with conventional direct-imaging techniques, there is a dramatic improvement in the ability to detect asteroid companions. Adaptive optics (1) decreases the light contribution from the primary asteroid at the position of the satellite on the plane of the sky and (2) increases the signal from the secondary at that position, enhancing the ability to detect, or set limits on the sizes of, satellites. In addition, because IR-imaging cameras are used, no charge bleeding (as for CCDs) occurs in an over-exposure of the primary. This effectively gives near-field coronagraphic imaging capability, allowing deep exposures for faint companions.

In adaptive optics systems, the light from the telescope is post-processed by a separate optical unit that resides beyond the telescope focal plane. A re-collimated beam impinges on a deformable mirror (DM), which has many actuators that can be adjusted rapidly to "correct" the beam back to its undistorted "shape". Light from the DM is then divided, with part (typically near-IR) of it going to the science camera, and part (typically visible) going to a wavefront sensor, which analyzes the deformation of the wavefront and provides correction signals to the DM, forming a closed loop.

Two types of systems are in use. One uses a Shack-Hartmann (SH) wavefront sensor, basically an  $x$ - $y$  array of many lenslets in a collimated beam. Each of these lenslets allows sensing of the beam deviation in a different part of the pupil. The other method is curvature-wavefront sensing (CS) (Roddier 1988) in which the wavefront sensor is divided in a radial/sectoral fashion. The illumination pattern of the beam is then sampled rapidly at positions on either side of a focal plane; the differences in illumination are related to the local wavefront curvature. While the Shack-Hartmann systems are more common, the curvature systems can work with fewer elements, at

faster speeds, and can work on fainter objects. CS systems trade the higher-order corrections of an SH system for faster (kHz) sample and correction speeds.

There are many AO systems either in use or under development. Among those that have been used for planetary applications are systems at Starfire Optical Range (U.S. Air Force), Mt. Wilson 100", University of Hawaii (on 88", UKIRT, and CFHT), Canada-France-Hawaii Telescope (CFHT), Keck, ESO/Adonis, Lick, Palomar, and Gemini North. Only three of these systems, all located on Mauna Kea, Hawaii, have resulted in discoveries of asteroid satellites. The 3.6m CFHT uses a 19-element CS system called PUEO (Roddier, Northcott, & Graves 1991; Rigaut *et al.* 1998). It can reach a limiting magnitude of about V=14.5 with a resolution of about 0.11 arcsec at H-band. The 10m Keck uses a 349-element SH system (Wizinowich *et al.* 2000), allowing compensation to about V=13 with a resolution of 0.04 arcsec at H-band. The 8.1m Gemini telescope, with the Hokupa'a 36-element CS system (Graves *et al.* 1998) of the University of Hawaii can reach about V=17.5, with resolution of about 0.05 arcsec at H-band.

The AO systems must have a reference point-source to compute the atmospheric turbulence. The systems may either use natural guide star (NGS) or an artificially-generated star (LGS), in which a laser is used to produce a point-source in the upper atmosphere. Laser-guide systems have largely been tested and used within military applications; although there are plans for LGS systems at many astronomical facilities, the progress has been slow and of limited use thus far. Therefore, NGS systems dominate AO systems. For astronomical (fixed-source) applications, a nearby brighter star may be used, provided it is within the isoplanatic patch, which may be about 20 arcsec at 2 $\mu$ m. But for planetary objects, *e.g.*, main-belt asteroids, their fast motion prohibits use of nearby objects, and one must rely on the object itself as the reference. This presents two limitations, one is that extended objects will tend to degrade the quality of the compensation, although asteroids are not extended enough to be of concern. Next, the quality of the AO correction depends upon the brightness of the reference object, so there is a limit to how faint an asteroid can be observed.

Most of the AO systems operate in the near IR, using HgCdTe IR (1–2.5  $\mu$ m) array detectors as the science camera. Although the ultimate signal-to-noise of the science data is a function of the brightness in the selected IR band, it is the visible light that is used by the wavefront sensor, so the quality of the AO compensation is dependent upon the V magnitude.

The correct wavelength band for observations is adjusted depending on conditions and the telescope. With IR AO observations, there is always a tradeoff between competing effects — the shorter the wavelength, the narrower the PSF for a given telescope. But at shorter wavelengths, the number of cells in the telescope beam that need to be continuously corrected grows beyond the capacity of the AO system — more cells require more AO actuators for compensation. But systems with a large number of actuators means prohibitively high cost, so there is a limit. Of course, the larger the telescope, the more number of cells to compensate. Therefore, the 10-m Keck usually performs best at K'-band (2.1  $\mu$ m) and the 3.6 m CFHT at H-band (1.6  $\mu$ m). Thus, the Strehl ratio (the ratio of peak brightness of acquired image to the peak brightness of a perfectly diffraction-limited point source) increases at longer wavelengths, while the instrumental width also increases. Under good conditions one hopes to achieve about 50% Strehl. On exceptionally good nights, it may be possible to use J-band (1.2  $\mu$ m) for a narrower PSF.

The future holds great promise for AO, as more telescopes adopt this technology. In addition, the advent of quality LGS systems and the opportunity for systems employing many more actuators, as costs decline and computer speeds increase, means the possibility of visible-light systems

and a correspondingly narrower diffraction limit.

Using AO, because the result is a picture of the system on the plane of the sky, we can hope to achieve the same information (and more) about a system as can be obtained from visual binary stars, only on a substantially shorter time scale. Basically, all 7 dynamic orbital elements required to describe the motion are derivable. These are the elements describing motion along the orbital ellipse: the semi-major axis, the eccentricity, and an indication of orbital phase, such as time of periape passage or true anomaly; plus the elements describing the orientation in 3-D space: e.g. the inclination, the longitude of the ascending node, and the argument of periape; in addition, because the system mass is unknown (unlike Sun-orbiting objects) we also require determination of the orbital period. From a limited span of observations, say a single orbit or series of a few orbits, there remains a 2-fold ambiguity in the orbital pole position (determination of the pole direction is equivalent to determination of the two elements inclination and node). But this can be resolved by observing at a different viewing geometry at some later time. The period and orbit size (assuming a circular orbit) are readily obtainable, which immediately yields an estimate of the system (primary + secondary) mass, by Kepler's Third Law. If the secondary is small or if we can independently determine the size ratio (and then make an assumption that the primary and secondary are of the same density) then the primary mass can be estimated. If the primary asteroid size is known, then we can determine the primary's density. Of course, density is clearly one of the most fundamental parameters one hopes to know about any body, and gives direct insight into the composition and structure. Because most of the orbits are small in angular terms (and pixels on a detector), the errors in measurement of positions translate into sizeable uncertainties in all of the orbital elements. However, the period can be very accurately determined, and the ultimate uncertainties in density are dominated by uncertainties in the size of the asteroid.

### 2.2.2 (45) Eugenia

The first binary system discovery using AO was accomplished on 1998 Nov 1 when a small companion of (45) Eugenia was discovered at the CFHT by Merline *et al.* (1999b, 1999c). The system was tracked for 10 days and again occasionally in following months and years. It was the first AO system for which the 2-fold degeneracy in the orbit pole had been resolved. Further, because of the large brightness difference (about 7 mag), it remains one of the more difficult AO-binaries to observe. Figure 4 shows the discovery image of this object, provisionally named S/1998 (45) 1, and was later given the permanent name Petit Prince, in honor of the prince imperial of France, the only child of Napoleon III and his wife Empress Eugenie (namesake of Eugenia). (The name itself is derived from the popular children's book *Le Petit Prince* by A. Saint-Exupery, whose central character was an asteroid-dwelling Little Prince.) The intention was to keep and solidify the tradition of naming asteroid moons after the children or other derivative of the parent asteroid. Figure 5 shows 5 epochs of the orbit at the time of discovery. Figure 6 exhibits the tremendous power of modern AO techniques to both resolve the asteroid and clearly separate a close companion.

The satellite appears to be roughly in the asteroid's equatorial plane, and it is in a prograde orbit (same sense as the primary spin) (Merline *et al.* 1999c). A prograde orbit is preferred for a satellite formed from impact-generated orbital debris (Weidenschilling *et al.* 1989, Durda & Geissler 1996). A retrograde orbit, however, is more stable against perturbing effects of the non-uniform gravitational field of an oblate primary (Chauvineau, Farinella, & Mignard 1993; Scheeres 1994). An orbit with an opposite sense to the asteroid's orbital motion around the Sun (as it is for Petit

Prince — Eugenia's spin is retrograde) is more stable against the effects of solar tides (Hamilton & Burns 1991). Mechanisms for capture of such ejecta into quasi-stable orbits is reviewed by Scheeres *et al.* (this volume).

The orbital period was determined to be about 4.7 days for the satellite of this FC-type asteroid and yields a density estimate of about  $1.2 \text{ g cm}^{-3}$  (Merline *et al.* 1999c). This result followed soon after the surprising announcement that the density to C-type Mathilde was only  $1.3 \text{ g cm}^{-3}$ , as determined by spacecraft flyby (Everka *et al.* 1999a). Such a density requires a significant amount of macroporosity to be consistent with the expected meteorite analog for these objects, namely carbonaceous chondrites (Britt & Consolmagno 2000). Therefore, it is possible that these asteroids are loosely-packed rubble piles.

### 2.2.3 (90) Antiope and (617) Patroclus

The first true double asteroid, (90) Antiope, was discovered in 2000 Aug by Merline *et al.* (2000a). This main-belt C-type was found to have two nearly equal-sized components of diameter about 85 km, rather than a single object of size 120 km, as was previously assumed. The orbital period of the pair was found to be about 16.5 hours, consistent with the previously observed lightcurve period. Interestingly enough, a lightcurve by Hansen *et al.* (1997) showed a classic eclipsing-binary shape (although they did not make this interpretation), which would be expected to result from equal-sized components, with the orbit viewed edge-on. The derived density for the components of (90), assuming they are of the same size and density, is about  $1.3 \text{ g cm}^{-3}$ , again similar to previous measurements of low-albedo asteroids. Figure 7 shows the components of Antiope as they orbit the common center-of-mass. Another double, (617) Patroclus, was discovered in 2001 Sep by Merline *et al.* (2001b). Again, it is primitive P-type, and is the first Trojan to be shown definitively to be binary. Few data were acquired but it appears that this object also will show a low density.

### 2.2.4 (762) Pulcova, (87) Sylvia, and (22) Kalliope

Small satellites were also found around two more large, low-albedo asteroids: F-type (762) Pulcova (Merline *et al.* 2000b), at CFHT, and P-type (87) Sylvia (Brown & Margot 2001), at Keck. Sylvia, a Cybele, is the first binary found in the outer Main-Belt. In Aug/Sep 2001, a small companion to (22) Kalliope was co-discovered by Margot & Brown (2001) and Merline *et al.* (2001a). This is the first M-type asteroid known to have a companion and gives the first hope of getting a density estimate for these controversial objects, which have traditionally been thought to be metallic. Initial estimates put the density between near about  $2.3 \text{ g cm}^{-3}$ . This value is even lower, although not significantly, than the values previously derived for S-types (around  $2.5 \text{ g cm}^{-3}$ ). If so, it clearly indicates that at least Kalliope is not predominantly of a solid metallic composition. It would also be difficult to imagine an extremely porous rubble-pile of metallic composition, because it would imply a macroporosity of more than about 60%. We may be faced with the difficult task of explaining how bodies with metallic spectra and radar reflectivities have rock-like densities.

### 2.2.5 (3749) Balam

Among the main-belt binaries, this object stands out as an oddity. Discovered at Gemini Observatory in 2002 by Merline *et al.* (IAUC 7827), this binary is the most loosely-bound system

known, even more so than the TNO binaries. The secondary appears to orbit at least 100 (primary) radii from the primary, which itself is rather small (about 7 km diameter). This is probably the first system known that was formed by “disruptive capture”, discussed in Section 3.3. Early models of Durda (1996) and Doressoundiram *et al.* (1997), as well as the more sophisticated models currently being performed by Durda *et al.*, indicate that such systems (small primaries, with a widely-separated secondary) are commonly formed in catastrophic collisions and that a large number of should be found in the Main Belt.

## 2.2.6 Systematics

While there appears to be a rash of newly discovered binaries, it turns out that the prevalence of (large) main-belt moons is likely to be low, probably approximately 2% (Merline *et al.* 2001d). The largest survey to date, of Merline *et al.*, has sampled over 300 main-belt asteroids, with 5 examples of relatively large satellites (few tens of km in diameter). The overall frequency, including small, close-in moons such as Dactyl (which are currently unobservable from Earth) will undoubtedly raise this, but it is unknown how much. Very small satellites will have a limited lifetime against collisions, although it is possible they may reaccrete. The single known binary among the Trojans, from a sample of about 6, hints that the binary frequency may be higher in that population, although it is noted that the collision speeds are comparable to the Main Belt and the collision frequencies are only higher by about a factor of two (Davis *et al.*, this volume).

For those satellites that are found, it would be useful to establish any systematics that may provide clues as to the origin mechanism for the moons. For example, it has been suggested that either slow (from tidal spin-down due to a satellite) or fast (from a glancing collision, which might form satellites) rotation might be correlated with the presence of satellites. Family members have been suggested as likely candidates for satellites, because co-orbiting pairs may have been created in the family-forming event. The likelihood of moons may even be linked to the taxonomic type or to the shape of the asteroid.

Most of the observed binaries in the Main Belt, outer-belt, or Trojan region are of primitive type (C, F, P). Are satellites truly more prevalent around these objects, or is there some observational selection effect? Clearly, those asteroids highest in priority for observation are the apparently brighter objects. Among the objects in Merline *et al.*’s target lists, the S-like and C-like asteroids are about equal in number. (This may mean that the frequency of binaries is more like 4% among the primitive asteroids.) But this is not where the bias ends. To be of equal brightness, a C-like asteroid must be much larger than an S-like, and therefore will have a larger Hill sphere. As such, one can image deeper into the gravitational well of a C-like object than an S-like object of the same apparent brightness, on average. Given that most of the observed companions reside within about 12 primary radii, the companions of C-like objects will be more easily found. Nonetheless, if the frequency of companions were also 4% for the S-like asteroids, some should still have been found. This raises the question as to whether it is more difficult to make satellites around S-types, which may be predominantly fractured-in-place chards, rather than rubble piles (Britt & Consolmagno 2001). If this is true, and because many of the outer-belt and Trojan asteroids are of primitive type, we may find ultimately a higher binary frequency among those populations.

Tables 1 and 2 summarize the properties of known binary systems discovered using adaptive optics or direct imaging techniques.

Table 1: **Binary asteroids discovered by adaptive optics or direct imaging techniques.**

Object	Type	Tax. Class (Tholen)	Family	Asteroid $a$ (AU)	Primary Rotation Period (h)	Primary Diam (km)	Discovery Date	Method
(243) Ida	MB	S	Koronis	2.86	4.63	31	1993 Aug 29	SC
(45) Eugenia	MB	FC	Eugenia	2.72	5.70	215	1998 Nov 01	AO
(762) Pulcova	MB	F		3.16	5.84	137	2000 Feb 22	AO
(90) Antiope	MB	C	Themis	3.16	16.50*	85+85	2000 Aug 10	AO
(87) Sylvia	OB	P		3.49	5.18	261	2001 Feb 18	AO
(107) Camilla	OB	C		3.48	4.84	223	2001 Mar 01	HST
(22) Kalliope	MB	M		2.91	4.15	181	2001 Aug 29	AO
(3749) Balam	MB			2.24		7	2002 Feb 08	AO
(617) Patroclus	L5-TROJ	P		5.23		95+105	2001 Sep 22	AO
1998 WW <sub>31</sub>	TNO			44.95		150**	2000 Dec 22	DI
2001 QT <sub>297</sub>	TNO			44.80		580 <sup>†</sup>	2001 Oct 11	DI
2001 QW <sub>322</sub>	TNO			44.22		200 <sup>‡</sup>	2001 Aug 24	DI
1999 TC <sub>36</sub>	TNO			39.53		740 <sup>†</sup>	2001 Dec 08	HST
1998 SM <sub>165</sub>	TNO			47.82	7.98	450 <sup>†</sup>	2001 Dec 22	HST
1997 CQ <sub>29</sub>	TNO			45.34		300 <sup>†</sup>	2001 Nov 17	HST
2000 CF <sub>105</sub>	TNO			44.20		170 <sup>†</sup>	2002 Jan 12	HST

**Notes for Tables 1 and 2:** \*assuming synchronous rotation; \*\*assuming, for both components, albedo  $\sim 5.4\%$  and density  $\sim 1 \text{ g cm}^{-3}$  (Veillet *et al.* 2002); <sup>†</sup>values provided by A.W. Harris (priv. comm.), assuming albedo 4%; <sup>‡</sup>assuming albedo 4% (Kavelaars *et al.* 2001); <sup>††</sup>this period is reasonable, despite the large observed separation, because of a high eccentricity (A.W. Harris, priv. comm.); MB = Main Belt; OB = outer belt; TROJ = Jupiter Trojan; TNO = Trans-Neptunian Object; SC = spacecraft encounter; AO = Adaptive Optics; HST = HST direct imaging; DI = Direct ground-based imaging.

Table 2: Properties of secondaries and derived properties of primaries.

Object	Orbit $a$ (km)	Orbit period (d)	Orbit size $a/R_p$	orbit sense	moon diam (km)	size ratio $D_p/D_s$	Primary mass $\times 10^{16}$ kg	Primary Density $\text{g cm}^{-3}$	mass ratio $M/m$
(243) Ida	108	1.54	7.0	prograde	1.4	22	4.2	$2.6 \pm 0.5$	11 000
(45) Eugenia	1190	4.69	11.1	prograde	13	17	610	$1.2 \pm 0.4$	4900
(762) Pulcova	810	4.0	11.6		20	7	260	$1.8 \pm 0.8$	340
(90) Antiope	170	0.69	4.0		85	1.0	41	$1.3 \pm 0.4$	1.0
(87) Sylvia	1370	3.66	10.5		13	20	1500	$1.6 \pm 0.3$	7900
(107) Camilla	~ 1000		~ 9		9	25			18 000
(22) Kalliope	1060	3.60	11.7	prograde	19	10	730	$2.3 \pm 0.4$	870
(3749) Balam	~ 350	~ 100	~ 100		1.5	4.6			95
(617) Patroclus	610	3.41	11.6		95	1.1	87	$1.3 \pm 0.5$	1.3
1998 WW <sub>31</sub>	22 300	574	300**		120**	1.2	170		1.7
2001 QT <sub>297</sub>	~ 20 000			69 <sup>†</sup>		1.4			2.6
2001 QW <sub>322</sub>	~ 130 000	~ 1500 <sup>††</sup>	1300 <sup>‡</sup>		200**	1.0			1.0
1999 TC <sub>36</sub>	~ 8000			22 <sup>†</sup>		2.8			21
1998 SM <sub>165</sub>	~ 6000			27 <sup>†</sup>		2.4			14
1997 CQ <sub>29</sub>	~ 5200			35 <sup>†</sup>		~ 1?			~ 1?
2000 CF <sub>105</sub>	~ 23 000			270 <sup>†</sup>		1.6			3.9

### 2.3 Discovery by Direct Ground-Based Imaging

Despite the difficulty of directly resolving a binary asteroid system from the ground without the assistance of adaptive optics, detections have been recently achieved. By direct imaging with CCDs on large telescopes, under conditions of exceptional seeing, it has been possible to resolve TNO binaries. Toth (1999) discussed some of the issues regarding detectability of these objects. The first of these, 1998 WW<sub>31</sub>, was discovered by Veillet *et al.* (2001, *IAUC 7610*) in 2000 December at CFHT. Follow up observations of 1998 WW<sub>31</sub> from ground-based telescopes and HST, as well as archival searches of previous data sets, indicate that the system has a size ratio of about 1.2, with an eccentric ( $\sim 0.8$ ) orbit, a semi-major axis near 22,000 km, and a period of about 570 days (Veillet *et al.* 2002).

Soon afterwards, two more TNO binaries were detected in the same way: 2001 QT<sub>297</sub> (Eliot *et al.* 2001, *IAUC 7733*), showing a separation of 0.6 arcsec at time of discovery and a size ratio of about 1.7; and 2001 QW<sub>322</sub> (Kavelaars *et al.* 2001, *IAUC 7749*) with a size ratio of about 1.0 and a wide separation of 4 arcsec when discovered. Four additional TNO systems were subsequently discovered using HST (discussed in Section 2.6). All of these systems, except one, are classical Kuiper Belt objects, residing at about 45 AU. One system, 1999 TC<sub>36</sub>, is a Plutino at about 40 AU.

For these objects, AO cannot be used directly because they are too faint, so direct imaging, either from the ground, or in ongoing campaigns on the HST, are likely to be the most attractive techniques. Because they move slowly past field stars, it is possible to use AO to image these objects during appulses with brighter stars. This technique may improve the overall sensitivity to fainter companions.

The size of the Hill sphere of an object is directly proportional to its distance  $r$  from the Sun, but the angular size of a satellite orbit, as seen from Earth is inversely proportional to the distance from the observer,  $\Delta$ , which is approximately  $r$ . So if satellites reside at the same fraction of their Hill sphere from the primary, there should be no advantage of direct imaging in observing outer solar system objects compared with similar-sized objects in the Main Belt. Apparently, the main reasons that these systems are being found with direct imaging, while those in the Main Belt are not, is that the secondary/primary size ratios are high, making the secondary easier to detect, while at the same time, the satellites are more loosely bound. Further, the TNO primaries are rather large, further assisting detection because of the correspondingly larger Hill sphere. Possibly, similar systems are rare in the Main Belt, and the TNO binaries are formed by a different process.

## 2.4 Radar discovery and characterization of binary NEAs

The radar instruments at Goldstone and Arecibo recently provided the first confirmed discoveries of binary asteroids in the near-Earth population (Margot *et al.* 2002a,b). In the 18-month period preceding this writing, five near-Earth objects have been unambiguously identified as binary systems: 2000 DP<sub>107</sub> (Ostro *et al.* 2000b; Margot *et al.* 2000); 2000 UG<sub>11</sub> (Nolan *et al.* 2000); 1999 KW<sub>4</sub> (Benner *et al.* 2001a); 1998 ST<sub>27</sub> (Benner *et al.* 2001b); and 2002 BM<sub>26</sub> (Nolan *et al.* 2002). Previous attempts to detect asteroid satellites with radar date back to the search for a synchronous moon around Pallas (Showalter *et al.* 1982). Ostro (priv. comm.) recalls that concrete anticipation for the radar discovery of binary systems arose with the imaging and shape modeling of the strongly bifurcated NEA (4769) Castalia (Ostro *et al.* 1990; Hudson & Ostro 1994). Ostro *et al.* (this volume) provide a thorough description of radar observations of asteroids.

In continuous-wave (CW) data sets, in which echoes resulting from a monochromatic transmission are spectrally analyzed, the diagnostic signature is that of a narrowband spike superposed on a broadband component. The wide-bandwidth echo is distinctive of a rapidly rotating primary object, *i.e.*, with spin periods of order a few hours. The narrowband feature, which does not move at the rate associated with the rotation of the primary, represents power scattered from a smaller and/or slowly spinning secondary. As time goes by, the narrowband echo oscillates between negative and positive frequencies, representing the variations in Doppler shift of a moon revolving about the system's center of mass (COM). The timescale associated with this motion in the small sample of objects studied so far is on the order of a day.

In delay-Doppler images, in which echo power is discriminated as a function of range from the observer and line-of-sight velocity, the signatures of two distinct components are easily observed. Both the primary and secondary are typically resolved in range and Doppler, and their evolution in delay-Doppler space is consistent with the behavior of an orbiting binary pair. Example data sets are shown in Figure 8.

The observables that can be measured from radar images are as follows: (1) visible range extents, which constrain the sizes of each component, (2) Doppler bandwidths, which constrain the spin periods of both the primary and secondary, (3) range and Doppler separations as a function of time, which characterize the system's total mass and orbital parameters, (4) reflex motion of the primary about the COM, which constrains the mass ratio of the system. Although the location of the COM is initially uncertain, the process of ephemeris refinement quickly leads to a very precise knowledge of its position in each image frame.

The bulk of the data analysis so far has concentrated on using the range and Doppler separations

to fit for the system's total mass and orbital parameters. The model assumes that the orbital motion of the secondary takes place in a plane with an orientation that remains fixed in inertial space during the time of the observations. Such mass estimates, coupled with a detailed knowledge of the component volumes from shape modeling techniques (Hudson 1993), can lead to precise asteroid density measurements. The density values presented here rely on size estimates from visual inspection of the raw radar images and on the verifiable assumption that most of the system's mass belongs to the primary object.

The current best-fit orbital parameters along with the formal errors of the fit are presented in Table 3. All solutions have chi-squared values  $\simeq 1$ . The best-fit mass and density estimates are also shown.

**Table 3: Binary asteroids detected by radar.**

Object	$a$ [m]	$e$	$P_{orb}$ [days]	$(M_1 + M_2)$ [ $10^9$ kg]	$R_p$ [m]	$R_s$ [m]	$a/R_p$	$\rho$ [g cm $^{-3}$ ]
2000 DP <sub>107</sub>	$2622 \pm 54$	$0.010 \pm 0.005$	$1.755 \pm 0.002$	$460 \pm 50$	$400 \pm 80$	150	6.6	$1.7 \pm 1.1$
2000 UG <sub>11</sub>	$337 \pm 13$	$0.09 \pm 0.04$	$0.770 \pm 0.003$	$5.1 \pm 0.5$	$115 \pm 30$	50	2.9	$0.8 \pm 0.6$
1999 KW <sub>4</sub>	$2566 \pm 24$	$\leq 0.03$	$0.758 \pm 0.001$	$2330 \pm 230$	$600 \pm 120$	$< 200$	4.3	$2.6 \pm 1.6$
1998 ST <sub>27</sub>	4000–5000				$250\text{--}300$	$< 50$	13–20	
2002 BM <sub>26</sub>			$< 3$		300	50		

Orbital parameters for radar-observed binary NEAs, including semi-major axis in meters, eccentricity, orbital period in days, and inferred total mass. Size and density estimates of the primary are also listed.

The binary systems observed with radar so far share similar characteristics. The primary components all appear roughly spheroidal and have spin periods near the breakup limit. The secondaries have diameters of order  $\frac{1}{3}$  the diameter of the primary, and their orbital and spin periods are consistent with spin-lock. All five radar-observed NEA binaries have satellites orbiting at a distance of a few primary radii. Their orbital period is on the order of a day. Because the spin periods of the primary are typically a few hours, the systems observed to date cannot be mutually synchronous. The spin periods of the secondaries are indicative of spin-lock configurations, which is consistent with calculations of tidal despinning timescales (Margot *et al.*, 2002b).

For 2000 DP<sub>107</sub> and 1999 KW<sub>4</sub>, one cannot reject the hypothesis that the orbit is circular, but for 2000 UG<sub>11</sub> that hypothesis can be rejected at better than the 1% level. The ability to determine the orientation of the orbital plane, using radar, depends critically on the plane-of-sky coverage. For 2000 DP<sub>107</sub>, which had a sky motion of  $\sim 40^\circ$  during the radar observations, the orientation of the orbital plane can be constrained to within a  $28^\circ$  cone. In the case of 2000 UG<sub>11</sub> and 1999 KW<sub>4</sub>, with  $\sim 60^\circ$  and  $\sim 110^\circ$  of sky motion respectively, pole solutions are expected to be better constrained.

Reflex motion of the primary is clearly observed in the radar data sets, providing the exciting prospect of measuring the densities of NEA satellites. Improved orbital fits will incorporate the residual motion of the primary with respect to the COM and will include the mass ratio of the system as an additional parameter.

The proportion of binary objects among radar-observed NEAs larger than 200 m is about 16%

(Margot *et al.* 2002b). This large proportion requires the formation of binaries to be frequent compared to the  $\sim 10$  Myr dynamical lifetime of NEAs. Radar observations show that binary NEAs have spheroidal primaries spinning near the breakup point for strengthless bodies, suggesting that the binaries formed by spin-up and fission, probably as a result of tidal disruption during close planetary encounters (Section 3.1).

Additional improvements are expected from shape reconstruction techniques (Hudson 1993), in which a series of delay-Doppler images are inverted in a least-squares sense to provide a shape model. Apart from possibly yielding clues on formation mechanisms, shape models will significantly decrease the uncertainties associated with size/volume estimates, and this will result in considerably lower error bars on the initial density measurements presented here. Given images with sufficient signal-to-noise ratio and orientation coverage, it may also be possible to infer shape and spin information for the satellites, and to derive solid conclusions regarding possible spin-orbit resonances.

The techniques for extracting information about binary systems from the radar data are still very much under active development. At this early stage, it appears that one weakness of the radar method lies in its inability to unambiguously constrain the orientation of the orbital plane, particularly when sky motion is limited. This is an intrinsic limitation of range and line-of-sight velocity measurements obtained without angular leverage. Observations over a range of aspect angles can overcome this ambiguity. The detection of occultations in the radar data or of occultations or eclipses from lightcurve observations can also place tight constraints on the inclination of the orbit. In general, a combination of radar and lightcurve observations will yield the best orbital determinations. The radar data may in turn help the interpretation of lightcurve profiles by distinguishing occultations from eclipses and primary from secondary events. Interesting synergies are therefore expected from the combination of the radar and lightcurve techniques. Because radar shadows are cast in much the same way as their optical counterparts, radar occultations of binary systems will be observed sooner or later, in which case the orientation of the orbital plane would be very tightly constrained. Radar+VLBA techniques (D.B. Campbell, priv. comm.) may also provide plane-of-sky images of close-approaching binary systems.

Radar observations of binary asteroids constitute an emerging field that holds great promise for the future. The information that can be gathered from radar data sets includes density measurements and orbital characteristics. Combined with high resolution imaging and shape models, these may provide powerful constraints on the formation mechanisms of binary NEAs. The characteristics of eccentricity and spin damping may also provide insightful clues about asteroid internal structure.

## 2.5 Binary Asteroids Detected by Lightcurves

Serious attempts to reveal binarity of some asteroids from their lightcurve features date back to the 1970s (*cf.* Cellino *et al.* 1985). A review of the advantages and disadvantages of various methods of extracting such information from asteroid lightcurves is given by Weidenschilling *et al.* (1989). Recent advances in methods for interpretation of lightcurves can be found in Kaasalainen *et al.* (this volume). While most techniques have not led to a successful detection of a binary asteroid so far, one of them, mentioned in the end of Section IV.B of Weidenschilling *et al.*, has been successful recently — detections of non-synchronous satellites.

Pravec (1995) analyzed a two-period lightcurve of the near-Earth asteroid 1994 AW<sub>1</sub>, measured

by Mottola *et al.* (1995) and Pravec *et al.* (1995), and interpreted the complex lightcurve as being due to occultation/eclipse events in a binary asteroid system combined with a fast rotation of the primary. The results were published also in Pravec & Hahn (1997), who presented the binary hypothesis as the likely explanation of the 1994 AW<sub>1</sub> lightcurve, but also considered the possibility that it might be an asteroid in a complex rotation state. In the light of more recent results (see below), the binarity of 1994 AW<sub>1</sub> is quite likely and we consider it to be the first binary asteroid detected by the lightcurve technique. See Table 4 for estimated parameters of this binary system.

The second binary asteroid found from lightcurve observations is 1991 VH (Pravec *et al.* 1998). Their extensive photometric observations show that the asteroid's lightcurve is doubly-periodic, that its long-period component shows occultation-like features, and they interpret the data as being evidence that 1991 VH is an asynchronous binary system, similar to 1994 AW<sub>1</sub>. The same or similar observational/analysis techniques have been used to reveal binarity in several other cases, which are shown Table 4. The general technique has been validated by the radar detection of the binarity of 2000 DP<sub>107</sub>, for which Pravec *et al.* (2000b) (and Pravec *et al.* 2002c, in preparation) observed a two-period lightcurve of the same kind as in the previous cases and estimated parameters of the binary system that are in agreement with results from the radar observations.

This lightcurve technique for detecting binaries has been described in the above mentioned papers as well as in more recent works by Pravec *et al.* (2000a) and Mottola & Lahulla (2000). Briefly, it is based on detecting brightness attenuations caused by mutual occultations or eclipses between components of the binary system that are superposed on the short period rotational lightcurve of the primary. An example is shown in Figure 9. The principles of the technique introduce several selection effects. The technique can reveal the existence of large satellites around asynchronously rotating primaries only under favorable geometric conditions. Another bias is that detection of close binary systems is favored, because observations and their interpretation are easier for systems with shorter orbital periods. Satellites smaller than about 20% of the primary diameter are difficult or impossible to detect unambiguously from lightcurve observations because they produce only small brightness attenuations during occultations or eclipses, less than about 0.04 mag. This may be difficult to separate from other effects, like an evolution of the primary's rotational lightcurve in changing observational geometric conditions. The asynchronous rotation of the primary allows one to resolve the occultation/eclipse events, which occur with a period different from the rotation period of the primary, and therefore rule out their possible connection with any peculiar shape feature of the primary. Occultations or eclipses can be observed only when the Earth or the Sun, respectively, lie close enough to the mutual orbital plane of the binary system. These selection effects mean that there may be a bias toward binary systems with certain favorable parameters in the sample of known or suspected binary asteroids presented in Table 4. Nevertheless, at least some of the similarities of the characteristics of the binary asteroids cannot be explained by selection effects alone and must be real.

The similarities of the 13 NEA binary asteroids, known or suspected from lightcurve or radar observations, are:

- They are small objects with primary diameters 0.7–4.0 km. The lower limit may be due to a bias against detection of small binary systems, because fainter asteroids are normally more difficult to observe. There may exist an upper limit but it is difficult to estimate from the small sample.
- They all are inner planet-crossers. Most of them approach the orbits of Earth and Venus.

This feature may be due, at least partly, to a selection effect, as km-sized asteroids are much easier to observe in near-Earth space than in the Main Belt. Another possible selection effect is that more observations are being made, in general, of near-Earth objects.

- All of the primaries are fast rotators (periods 2.3–3.6 h), not far below the critical stability spin rate, with low amplitudes (0.1–0.2 mag), suggesting nearly spheroidal shapes (see Pravec *et al.*, this volume).
- The secondary-to-primary diameter ratios are almost all in the range 0.2–0.6. While the lower limit may be just a result of the selection effect mentioned above, it appears that binaries with nearly equal-sized components are rare among km-sized NEAs. The probability that there are twelve objects with the diameter ratios in the range 0.2–0.6 and one in 0.6–1.0, for a uniform distribution of the diameter ratios, is less than 0.2%.
- Semi-major axes estimates are in the range 3.4–6.6 primary radii. While the upper limit may be due to the selection effect mentioned above, the lower limit (corresponding to orbital periods  $\sim 14$  h) may be real and it suggests that very close binary systems are not present (perhaps due to their instabilities).
- Eccentricities are poorly constrained but appear to be low, less than 0.1.

Pravec *et al.* (1999) accounted for the bias due to the selection effect related to the geometric observing conditions and estimated, on the basis of the first three known binary NEAs, that the fraction of binaries among NEAs is  $\approx 17\%$  with an uncertainty of a factor 2. This is consistent with the estimates from radar data that about 16% of NEAs are binary (Margot *et al.* 2002b), and the estimates (about 15%) of Bottke & Melosh (1996a,b) from models of binary production by tidal disruption (see Section 3.1). Based on these studies, we adopt 16% as our working estimate of the NEA binary fraction. We note that about 30% of km-sized asteroids are fast rotators with periods  $< 4$  h, and also that binary NEAs have fast-rotating primaries. Therefore, it may be that roughly half of the fast-rotating NEAs are binary (Pravec & Harris 2000) and that binary asteroids are common among fast-rotating objects on Earth-approaching orbits.

## 2.6 Hubble Space Telescope (HST) Companion Searches

One of the major projects that Zellner *et al.* (1989) expected to be addressed by HST was the search for asteroid companions. The absence of atmospheric effects on HST images allows diffraction-limited operation over a very large field of view. The spherical aberration of the primary mirror did not stop the execution of an early attempt to survey the asteroid belt (program 4521) as well as an “amateur” program that targeted asteroids thought to have companions, primarily from occultation observations (program 4764). No companions were found but careful restoration of the data was necessary to minimize the effects of the aberration. While aberration did not limit the spatial resolution of the images (the middle  $\frac{2}{3}$  of the primary was ground correctly) the additional “skirt” of scattered light did limit the dynamic range over which a companion could be detected.

Storrs *et al.* (1999a) published the data from these two programs. Their reconstruction of the HST images allowed upper limits to be put on the presence of companions to asteroids (9) Metis, (18) Melpomene, (19) Fortuna, (109) Felicitas, (146) Lucina, (216) Kleopatra, (434) Hungaria, (532)

**Table 4: Estimated Parameters of Binary NEAs, Detected by Lightcurve**

Object	$D_p$ [km]	$D_s/D_p$	$a/R_p$	$e$	$P_{orb}$ [h]	$P_{rot}$ [h]	$A_{rot}$ [mag]	Taxon. Class	Orb. Type	Ref. <sup>†</sup>
1994 AW <sub>1</sub>	0.9	0.53	4.6	< 0.05	22.40	2.5193	0.16		PHA	[1]
1991 VH (3671)	1.2	0.40	5.4	0.07	32.69	2.6238	0.11		PHA	[2]
1996 FG <sub>3</sub> (5407)	1.4	0.31	3.4	0.05	16.14	3.5942	0.09	C	PHA, VC	[4,5]
1998 PG	0.9	$\geq 0.30$	(3.4)	(< 0.05)	(13.52)	2.5488	0.13	(S)	MC	[4]
1999 HF <sub>1</sub>	3.5	0.24	4.0		14.02	2.3191	0.13	EMP	Aten, VC	[6]
2000 DP <sub>107</sub>	0.8	0.38	6.6	0.01	42.2	2.7755	0.22	C	PHA	[7,8,9]
2000 UG <sub>11</sub>	0.23	$\geq 0.6$	3.6	0.12	18.4	(4.44)	0.10	QR	PHA	[14,16]
1999 KW <sub>4</sub>	1.2	$\geq 0.3$	4.2	$\leq 0.03$	17.45	2.765	0.13	Q	PHA, VC	[10,11,14,15]
2001 SL <sub>9</sub>	1.0	0.31	3.6		16.40	2.4003	0.09		Apollo	[17]

The diameter of the primary  $D_p$  was estimated from the effective diameter 1.0 km given by Harris & Davies (1999) for (3671), and from measured absolute magnitudes assuming the geometric albedo  $p = 0.06$  for 1996 FG<sub>3</sub>, and 2000 DP<sub>107</sub>, and  $p = 0.16$  for the other objects; it was corrected for  $D_s/D_p = 0.4$  in cases where only a lower limit on the secondary-to-primary diameter ratio is available.  $a$  is the semi-major axis of the mutual orbit,  $e$  is its eccentricity,  $P_{orb}$  is the orbital period,  $P_{rot}$  is the rotation period of the primary,  $A_{rot}$  is its amplitude corrected for contribution of the light from the secondary. The values in brackets are derived using the assumptions discussed in Pravec *et al.* (2000a). PHA stands for potentially hazardous asteroid, which is an object approaching closer than 0.05 AU to the Earth's orbit, VC stands for Venus-crosser, MC stands for Mars-crosser. This table has been updated from Pravec *et al.* (2000a). For uncertainties and assumptions made with the estimates, see the original publications. Note that some of these objects are in common with NEAs observed by radar, in Table 3. An updated, combined radar/lightcurve NEA table is maintained at <http://www.asu.cas.cz/~asteroid/binneas.htm>.

<sup>†</sup> References: [1] Pravec & Hahn (1997); [2] Pravec, Wolf, & Šarounová (1998); [3] Mottola *et al.* (1997); [4] Pravec *et al.* (2000a); [5] Mottola & Lahulla (2000); [6] Pravec *et al.* (2002a); [7] Margot *et al.* (2002b); [8] Pravec *et al.* (2000b); [9] Pravec *et al.* (2002c), in preparation; [10] Benner *et al.* (2001a); [11] Pravec & Šarounová (2001); [12] Harris & Davies (1999); [13] Pravec, Wolf, & Šarounová, 1997, unpublished; [14] Margot *et al.* (2002a); [15] Pravec, P., Holliday, B., Šarounová, L., Goretti, V., Kusnirak, P., Wolf, M., Hicks, M.D., Krugly, Yu.N., Masi, G., & Vanmunster, T. (2002c), in preparation; [16] Pravec, P., Šarounová, L., Kusnirak, P., Hicks, M.D., Scheirich, P., & Wolf, M. (2002b), in preparation; [17] Pravec, Kusnirak, & Warner (2001).

Herculina, (624) Hektor, and (674) Rachele. No companions were found to a brightness limit that varied with distance from the primary, shown in Figure 10. Barring the companion being in conjunction at the time of observation, Storrs *et al.* rule out companion objects (suggested by early occultation observations) to asteroids (9) Metis, (18) Melpomene, and (532) Herculina (the brightness and separation of suggested companions are designated by the numbers in Figure 10).

No companions were found to the eight asteroids that were imaged by HST with the corrected Wide Field Planetary Camera 2 (WFPC2) instrument, as part of program 6559 (Storrs *et al.* 1998, 1999b). Further HST imaging observations are currently under way in program 8583, which is a “snapshot” program designed to fill in gaps in the spacecraft’s calendar of observations. The program targets 50 large, main-belt asteroids (many of them twice) with the WFPC2 in a manner similar to that used to map (4) Vesta by Binzel *et al.* (1997). This program resulted in the discovery of a companion to (107) Camilla (*IAUC 7599*), and confirming observations of the companions to (87) Sylvia (*IAUC 7590*) and to (45) Eugenia. The companions to (45) Eugenia and (107) Camilla have the same color in the visible range as their primaries. In *IAUC 7590*, Storrs *et al.* report that the companion to (87) Sylvia appears significantly bluer than its primary. The observations of (6) Hebe in this program show no companions brighter than seven magnitudes fainter than the primary, or larger than 8 km in diameter.

Another program to observe main-belt asteroids is that of Zappalà *et al.*, which used the HST Fine Guidance Sensor (FGS). The first results of this program confirmed that (216) Kleopatra is a contact binary (Tanga *et al.* 2002). Two other programs are underway, both of them targeting TNOs, and both began to detect binaries in early 2002. A large program by M. Brown has detected two TNO companions: 1999 TC<sub>36</sub> (Trujillo & Brown 2002, *IAUC 7787*) and 1998 SM<sub>165</sub> (Brown & Trujillo 2002, *IAUC 7807*). In a second program, two more binaries have been found: 1997 CQ<sub>29</sub> (Noll *et al.* 2002a, *IAUC 7824*) and 2000 CF<sub>105</sub> (Noll *et al.* 2002b, *IAUC 7857*). As in the case of the other known TNO binaries, these objects have a wide separation and have relatively large secondaries.

The strengths and weaknesses of HST/WFPC2 observations of asteroids are discussed in the chapter on “Observations from Orbiting Platforms” by Dotto *et al.* (this volume). Briefly, WFPC2 observations allow diffraction limited observation over a large field of view from the vacuum UV to beyond 1  $\mu\text{m}$  wavelength. These high resolution images can provide information on the shape and mineralogical variegation of the primary as well. Drawbacks include the robotic nature of HST scheduling (ephemerides good to better than 10 arcsec for over a year are necessary to find the asteroid), no sensitivity beyond 1  $\mu\text{m}$  (but see the discussion of WF3, which will operate to 1.8  $\mu\text{m}$ , in the chapter by Dotto *et al.* ), and the difficulty in getting time on HST (no immediate follow up of detections). HST observations are complementary to ground-based AO observations because they cover a larger field-of-view per exposure, at a shorter wavelength, but cannot cover the critical near-IR wavelength region.

## 2.7 Role of Occultations

Described as a technique of searching for asteroid satellites by Van Flandern *et al.* (1979) in *Asteroids I*, the method of using stellar occultations suffers from the inability to plan or repeat an experiment, at least reliably. Reitsema (1979) has called into question many of the early reports of satellites, indicating that the measurements are susceptible to spurious events. One-time reports of occultations can only serve to alert more rigorous search methods of a potential candidate. In

addition, once an asteroid is known to have a moon, systematic networks of observers may be placed so as to attempt to see an event from the moon, during an occultation of the primary. These observations could greatly constrain our understanding of the sizes and positions of the satellites.

It is important to note, however, that archived occultation records (D. Dunham, priv. comm.) have shown that 2 short events have been recorded accompanying an occultation of Eugenia (diameter 215 km). One was in 1983 (chord equivalent  $\sim$  9 km) and another in 1994 (chord equivalent  $\sim$  20 km). Another short event, of chord size 18 km, was recorded in 1997 during an occultation of Sylvia (diameter 271 km). The satellite diameters predicted from AO observations are 13 km for Eugenia and 13 km for Sylvia. It is unlikely that such short chords would have resulted from asteroids of this large size. Therefore, it is possible that these occultations in fact did record satellite events.

### 3 ORIGIN AND EVOLUTION OF BINARY ASTEROIDS

In *Asteroids II*, Weidenschilling *et al.* (1989) gave a discussion of the most promising mechanisms for formation of asteroid binaries. Most of the progress since that time has been observational, but theoretical efforts, especially numerical modeling, have also made advances. With the new examples of actual binary systems to study, there has recently been a renewed interest in theories of formation and in numerical modeling of binary origin. All of the formation mechanisms discussed by Weidenschilling *et al.* remain viable. Here we revisit these, and add others.

#### 3.1 NEAs: Tidal Encounters

As discussed in Sections 2.4 and 2.5, a significant fraction (16%) of NEAs appear to be binary. This is much higher than their apparent abundance in the Main Belt (although detection is more difficult for the latter), but is consistent with the fraction of recognized doublet craters in impacts on Earth (Weidenschilling *et al.* 1989). Apparently, some mechanism favors production of binaries among planet-crossers (unless it is possible to get small main-belt binaries to be ejected from the Belt intact). A close planetary encounter can subject an asteroid to tidal stresses and torques that may produce a binary. The same process, however, can also disrupt existing binary systems. Because the lifetime of near-Earth asteroids is relatively short (a few times  $10^7$  years), and close encounters are more probable than planetary impacts, this formation/destruction is an equilibrium process. Bottke & Melosh (1996a,b) first examined the effect of planetary encounters on contact binaries (two components), and concluded that  $\sim 15\%$  of Earth-crossers evolved into co-orbiting binaries. Richardson, Bottke, & Love (1998) and Bottke *et al.* (1999), modeled the tidal disruption of ellipsoidal shaped rubble-pile asteroids (composed of many small, equal-sized particles) encountering the Earth, and found that rotational spin-up frequently caused them to undergo mass shedding. In many cases, some of the shed fragments went into orbit around the progenitor, producing binary asteroids. Most of these satellites, however, were much smaller than the primary. Also, the yield of binaries was low; disruption into a string of clumps, as for comet Shoemaker-Levy 9, was more probable than binary formation. The results of these studies suggest that tidal disruption can produce enough binaries to account for the observed population of doublet craters on the terrestrial planets, provided that small asteroids (less than a few km in diameter) are not finely divided gravel piles, but “coarse” structures dominated by a few large chunks. This inference is also consistent with their observed maximum rotation rates (*cf.* Paolicchi *et al.*, this volume).

## 3.2 Cratering Ejecta

A cratering event from a sub-catastrophic impact on an asteroid produces ejecta with a range of velocities. It is likely, therefore, that some of the ejecta will have sufficient kinetic energy and angular momentum to go into orbit about the target body. Except in highly oblique impacts, the ejecta leaves the crater with a more or less uniform azimuthal distribution as seen in the frame of the target's surface. If the target is rotating, the rotational velocity of the surface at the impact point is added to the ejecta velocity; therefore, more mass will attain orbital velocity in the prograde direction (we assume that the impact is not large enough to make a significant change in the target's rotational state). The problem with this model is how to place the ejecta into stable orbits. If the target is a sphere with a purely radial gravity field, then the ejecta particles have elliptical orbits that would intersect its surface after one revolution. Collisions between fragments, and solar perturbations acting on particles with highly eccentric orbits, might prevent immediate re-impact, but these mechanisms would have to act during the first orbit after the impact, and appear to be inefficient. However, many asteroids are significantly non-spherical (triaxial) in shape and usually rotate about their shortest axis. This means that ejecta particles experience a non-central gravity field, which can significantly alter their orbital parameters on the timescale of a single orbit. Also, a particle launched from a point near the longer equatorial axis may encounter a shorter axis during its first few periapse passages, avoiding impact and prolonging its lifetime. Mutual collisions among fragments during the first few orbits can damp their eccentricities, yielding orbits that no longer intersect the primary's surface. This material could then accrete into a small satellite.

As pointed out by Weidenschilling *et al.* (1989), ejecta velocities must be within the limited range that allows material to go into orbit about the primary, without escaping completely. Such orbits have specific angular momentum corresponding to circularized orbits within a distance of about two radii from the primary. Unless this distance is outside the synchronous point, any satellite that accreted in this manner would be subject to tidal decay, and would eventually collide with the primary. The requirement that the synchronous distance lies within two radii implies a spin period of not more than about 6 hours. Tidal torque would then cause the satellite to migrate outward; for small secondary/primary mass ratios, the primary's spin would not be slowed significantly. Thus, satellites formed by this mechanism would be small rubble piles, in prograde orbits about rapidly rotating primaries. In addition to these criteria listed by Weidenschilling *et al.*, we add the requirement that the primaries be significantly non-spherical.

In a preliminary numerical study to explore the viability of this mechanism for producing small satellites, Durda & Geissler (1996) examined the accretion of ejecta particles from three different 10-km-scale craters on Ida. In each case they followed the dynamical evolution of 1000 ejecta particles for 100 hours after the cratering impact and searched for “collisions” between orbiting particles, treating each “collision” as an accretion event. That study found that temporary aggregates containing about 0.1% of the ejected debris mass did indeed form while in flight around the primary, but none of these aggregates occupied stable orbits and survived (although the temporary aggregates were primarily on prograde trajectories concentrated near the equatorial plane of Ida, as predicted by Weidenschilling *et al.* 1989). The failure of the model to yield small satellites via accretion of ejected cratering debris may not be evidence that this mechanism fails to work or is incredibly inefficient, but instead may fundamentally be a result of the approximations inherent to the model (the Dactyl-forming impact may also have been larger than modeled). Indeed, several processes that have subsequently been shown to play important roles in placing material into

bound orbits (*e.g.*, distortion of the primary's shape, vaporization of some fraction of material, impact angle) were not included in the modeling. Instead, the Durda & Geissler model, which has proven quite successful in explaining the distribution of ejecta on Ida's surface (Geissler *et al.* 1996), simulated the ejection of crater debris from various locations on Ida by launching particles from a point at a 45° angle to the local surface. The particles were all launched at the same instant at the beginning of the simulations, with no momentum transfer to the asteroid. In reality, excavation flows encompass the entire center-to-rim extent of a crater, the time scale for crater excavation on a low-gravity object can approach a significant fraction of the asteroid rotation period, and translational and rotational momentum is imparted to the primary during the impact (*e.g.*, Asphaug *et al.* 1996; Love & Ahrens 1997). Thus, a combination of shape/distortion effects and translational/rotational motion during the excavation phase may play an important role in allowing particles to remain in temporary orbit.

This mechanism would operate in the environment of high-velocity impacts in the present Main Belt. Impacts are also capable of destroying small satellites, which would have shorter lifetimes against disruption than their primaries (although they might reaccrete after such events if the fragments remain in orbit). Thus, we expect the population of such binaries to be in equilibrium between formation and destruction by impacts.

Of the main-belt asteroids known to be binaries, six of eight (22, 45, 87, 107, 243, and 762) have satellites much smaller than their primaries. Assuming equal albedos and densities for both components, the mass ratio is typically  $\sim 10^{-3}$ . Significantly, all of the primaries are rapid rotators; the longest period is 5.84 hours for (762) (Davis 2001). Also, they have rather large amplitude lightcurves, with maximum observed amplitudes of at least 0.25 mag. These properties are consistent with formation of their satellites from impact ejecta. If the direction of an orbit relative to the rotation of the primary is found to be prograde, this would be a strong indication of their origin by this mechanism. The sense of the orbit is known for three of these main-belt binaries. The moons of (243) Ida (Belton *et al.* 1995, 1996), (45) Eugenia (Merline *et al.* 1999b,c), and (22) Kalliope orbit in a prograde sense.

### 3.3 Disruptive Capture

Many asteroids belong to dynamical families that reveal them to be fragments of larger parent bodies that were disrupted by catastrophic collisions. In such a disruptive event, fragments may end up in orbit about each other, as suggested by Hartmann (1979). Weidenschilling *et al.* (1989) pointed out that in a radial velocity field of fragments escaping from a disrupted primary, geometrical constraints imposed by the finite sizes of fragments would tend to ensure that they would have relative velocities exceeding their mutual escape velocity, and in general would not remain gravitationally bound.

This problem was examined in some detail by Durda (1996) and by Doressoundiram *et al.* (1997), who simulated disruptions numerically, integrating orbits of fragments in the debris field. They found that the fraction of binaries depended on the magnitude of a random velocity dispersion assumed to be imposed on the general expansion; however, even with no dispersion some binaries were produced, apparently by jostling among fragments. More pairs of fragments in contact were produced than orbiting binaries. The fraction of contact pairs and binaries was small in Durda's models (about 0.1%), while the fraction of binaries found by Doressoundiram *et al.* was about 1%. The limited range of sizes and numbers of particles in the simulations probably limited the binary

fraction. Treating larger numbers of smaller fragments would be expected to yield more binaries with smaller satellite/primary mass ratios.

The early, simple numerical models of this mode of satellite formation contained some critical limitations, however. Because the initial conditions simulating the expansion phase following a catastrophic impact were merely treated in a simple empirical fashion, a self-consistent description of the mass-speed distribution of fragments and the direction of fragment ejection was not possible. Variations in these collision outcomes, and therefore in the efficiency of binary pair formation, with initial conditions, could not be examined in these initial studies. The next generation of numerical models (Michel *et al.* 2001; Durda *et al.* 2001) substantially improve upon the limitations of the Durda (1996) and Doressoundiram *et al.* (1997) models by conducting detailed 3-dimensional smooth-particle hydrodynamics (SPH) models of catastrophic collisions between asteroids (*e.g.*, Benz & Asphaug 1995; Asphaug *et al.* 1998), and then following the subsequent dynamics of the ejected fragments through fast, state-of-the-art N-body simulations (such as described in Leinhardt, Richardson, & Quinn 2000).

One of the most important benefits of this scheme over the previous numerical studies is that it includes a rigorous treatment of the impact physics, so that accurate fragment size distributions and velocity fields are established early in the ejection process. Thus, the dependence of satellite formation efficiency with respect to various collision parameters (*e.g.*, speed, impact parameter, impact angle) can be studied in a self-consistent manner. These new models also allow a far faster N-body integration scheme with efficient mutual capture and collision detection capabilities. A sample model can be seen in Figure 11.

Three of the known main-belt binaries (45, 90, and 243) are members of dynamical families, so this mechanism is plausible (however, the fraction of binaries in families does not appear to be greater than for the general population). There should be no initial preference for rapid rotation of primaries or prograde orbits, but tidal dissipation could cause loss of satellites of slow rotators or in retrograde orbits. We would expect no correlation with the primary's shape, so lightcurves may discriminate between cratering ejecta and disruptive capture.

### 3.4 Collisional Fission

An impact may shatter an asteroid without disrupting it. As the probability of an exactly central collision is zero, it will also impart angular momentum to the target. If the specific angular momentum exceeds a threshold value, a weak (shattered) self-gravitating body cannot remain single, but must fission into a binary, with some of the angular momentum in orbital motion rather than rotation. The angular momentum imparted is proportional to the impact velocity  $v$ , while the impact energy scales as  $v^2$ . As discussed by Weidenschilling *et al.* (1989), it is difficult to impart enough angular momentum without destroying the target at typical impact velocities ( $\sim 5 \text{ km s}^{-1}$ ) in the present Belt (although there is a distribution of velocities over a wide range, but at lower impact probabilities). If gravitational binding dominates, then for impacts large enough to impart the critical angular momentum, the ratio of impact energy to binding energy is of order  $v_{\text{impact}}/v_{\text{escape}}$ . For even the largest asteroids, disruption is more likely than rotational fission in the present collisional environment. Conditions were presumably more favorable in the earliest stage of the Belt's evolution, before velocities were pumped up; however, only large satellites would have been able to survive its later collisional history. No convincing candidate systems have yet been found in the Main Belt.

The masses and relatively large separation (about 4 radii) of the main-belt double (90) Antiope imaged by Merline *et al.* (2000a, 2000b) means that this pair has unusually high specific angular momentum. The lightcurve eclipses recorded by Hansen *et al.* (1997) are consistent with the nearly equal-sized components seen in the images. At other times, the lightcurve had a low amplitude consistent with nearly spherical, non-eclipsing components (actually, Darwin ellipsoids are an even better match). Merline *et al.* inferred a density of  $\sim 1.3 \text{ g cm}^{-3}$ , which suggests that the Antiope components may be “rubble piles” with equilibrium shapes. Such models of equilibrium binaries and the expected lightcurve morphologies were studied by Leone *et al.* (1984). The origin of the Antiope binary is hard to explain. It is a member of the Themis family, and so must postdate the disruption of its parent body by a high-velocity impact. Disruptive capture of two equal-mass fragments of such large size in that event is unlikely, and they would have to be converted to rubble piles by later impacts. However, some of the model runs of Michel (priv. comm.) appear to have produced similar-sized components. Collisional fission seems to be the most likely origin for Antiope, but still presents the problem of imparting so much angular momentum in a collision without dispersing the target. Due to the low orbital inclination of the Themis family, collisions between members have a lower mean velocity ( $\sim 3 \text{ km s}^{-1}$ ; Bottke *et al.* 1994) than between field asteroids ( $\sim 5 \text{ km s}^{-1}$ ) but this difference is not very significant. Weidenschilling *et al.* (2001) estimate that the required angular momentum implies an impactor of diameter  $\sim 20 \text{ km}$  on a 100 km target body, with about 100 times its gravitational binding energy, at the mean encounter velocity. An impact by a larger body at much lower velocity is improbable, even if the Themis family is several Gyr old. Low-velocity impacts could have occurred in the immediate aftermath of the disruption of the Themis family’s parent body, before Jovian perturbations randomized the nodes and apsides of the fragments. Models by Dell’Oro *et al.* (2002) show an enhancement in the impact probabilities of several orders of magnitude initially after breakup. However, the time available before randomization is short ( $\sim 10^4$  orbital periods), and a collision between two fragments of sufficient size is unlikely. In either scenario, the probability of forming a binary with these properties is only  $\sim 10^{-3}$ , and thus Antiope should be unique in the Main Belt.

### 3.5 Primordial Binaries?

Other binaries with components of comparable mass and large separations have been discovered, but at larger heliocentric distances. The Trojan asteroid (617) Patroclus (Merline *et al.* 2001b) and at least two of the TNO binaries (1998 WW<sub>31</sub>, 2001 QW<sub>322</sub>) have size ratios close to one. All have significantly greater separations than Antiope; about 600 km ( $\sim 12$  radii) for Patroclus and  $10^4$ – $10^5$  km ( $\sim 10^2$ – $10^3$  radii) for the TNOs. In one sense, these properties are not surprising; detection of smaller and/or closer satellites of such distant objects is impossible by currently available technology. However, it is unclear how such loosely bound pairs could have formed. If the Patroclus binary formed by a collision, it would have required more extreme parameters (larger impactor and/or lower velocity) than Antiope’s formation. The collision rate in the Trojan clouds is somewhat higher than in the Main Belt (see Davis *et al.*, this volume), while the mean impact velocity is comparable (lower orbital velocity is offset by higher mean inclination). However, a binary of this size would have a collisional lifetime greater than the age of the solar system. It is plausible, therefore, that the Patroclus binary formed by a low-velocity collision before eccentricities and inclinations were pumped up, perhaps before its capture into resonance with Jupiter.

The frequency of trans-Neptunian binaries appears to be of order 1%. Their large separations

could not have been produced by two-body collisions or tidal evolution. The most plausible origin for such a loosely bound binary seems to be an impact or gravitational encounter with another body of comparable mass while the two components passed within their mutual Hill radius. The present spatial density in the Kuiper Belt is far too low for 3-body encounters; any such events must have occurred when it was more populous and/or dynamically “cold” with low inclinations. Dynamical modeling is needed to determine the efficiency of binary production by this mechanism as a function of population density and orbital parameters. Alternatively, these binaries may represent objects that formed as loosely-bound pairs from inherent disk instabilities during accretion (S.A. Stern, priv. comm.). Observations of binary TNOs will eventually allow direct determination of their masses and densities, but may also provide a constraint on the formation and early history of the Kuiper Belt.

### 3.6 Tidal Evolution of Spins and Orbits

Weidenschilling *et al.* (1989) considered the tidal evolution of orbits of asteroidal satellites. Their Figure 1 showed the timescale for a hypothetical satellite to evolve outward from an orbit initially close to a primary of radius  $R = 100$  km, as a function of the satellite/primary mass ratio. There are now enough data for real binaries to compare this model with observation. Most of the known main-belt binaries have separations  $a/R \sim 10$ , and  $M/m \sim 3 \times 10^2 - 10^4$  (Table 2); the inferred tidal evolution timescales are in the range  $\sim 10^8 - 10^9$  yr. These values depend on the mechanical properties of the primaries, which are uncertain, but are consistent with collisional production of close binaries and tidal expansion of their orbits to their present distances since the formation of the asteroid belt. All such satellites lie below the line of synchronous stability, with orbits that are still evolving outward (consistent with the observation that their primaries have rotation periods shorter than their orbital periods). The NEAs typically have smaller separations with  $a/R \sim 5$ , and smaller  $M/m \sim 10^1 - 2 \times 10^2$ . However, they are much smaller than the main-belt binaries, with  $R \sim 1$  km; since the rate of tidal evolution of orbits scales as  $R^2$ , they also have timescales  $\sim 10^9$  yr, consistent with the observation that they have not evolved to a synchronous end-state. The binaries with relatively close massive satellites have much shorter evolution times; extrapolating from Weidenschilling *et al.*’s Figure 1, (90) Antiope would have reached its tidally locked end state in only a few thousand years, and (617) Patroclus in less than  $10^6$  yr. However, it can be seen from that figure that Patroclus has too much angular momentum to have evolved by despining of an initially close binary. This system, and the Kuiper Belt binaries with comparable mass ratios and still larger separations, must have attained their present orbital configurations by a mechanism other than tidal despining.

The timescale for despining of a satellite’s rotation by tides is generally shorter than that for evolution of its orbit by despining of the primary. Using the classic formula for the rate of despining (Goldreich and Soter 1966), the smaller main-belt and NEA satellites have despining times  $\sim 10^6 - 10^7$  yr, so they are expected to keep one face toward their primary. The only observational datum for rotation of a main-belt satellite is from the *Galileo* flyby of Ida/Dactyl, which showed that Dactyl had slow rotation, consistent with spin-orbit synchronicity (Everka *et al.* 1996b). On the other hand, the known Kuiper Belt binaries have such large separations that their tidal despining times probably exceed the age of the solar system; they are unlikely to be in synchronous rotation.

Finally, Harris (2002) has suggested that the gravitational ejection of a satellite from orbit

around an irregularly-shaped primary would deplete the rotational energy of the primary, thus slowing substantially the spin of the primary. This ultimately may be shown to be the cause of the anomalously slow rotation of many asteroids, which so far have eluded satisfactory explanation.

### 3.7 Triple and Multiple Systems

Little work has been done specifically to study the formation and stability of triple or multiple asteroid systems. Perhaps the closest analogues are those studies of stability of satellites around a non-spherical primary (*e.g.*, Scheeres 1994; Petit *et al.* 1997). Significant progress, however, has been made in the understanding of triple or multiple star systems. Many of these results can be applied directly to asteroids, to give insight into what characteristics might be expected for multiple-asteroid systems. It is generally accepted that the masses would be configured in a hierarchical fashion (*cf.* Eggleton & Kiseleva 1995). This would be a superposition of two binary systems: an inner massive object, orbited by a satellite and a moon of the satellite (like Sun/Earth/Moon) or a close binary system, with a tertiary object in a wide orbit about the central pair. The ratio of the semi-major axes of the two relevant “binaries” must be  $\sim 3\text{--}4$  to be stable (Harrington 1977a, 1977b). For eccentric orbits, the ratio of the periapse of the outer orbit to the inner semi-major axis is the relevant parameter. Eccentric orbits are therefore less stable (Eggleton & Kiseleva 1995; Kiseleva, Eggleton, & Orlov 1994). In addition, the stability depends, in a complicated way, on the mass ratios of the objects (Black 1982). Systems that have the two orbits counter-revolving (retrograde) also display greater stability than if the orbits are both in the same sense (Harrington 1977b). Recent work on evolution of triple systems (Miller & Hamilton 2002) emphasizes the importance of Kozai resonances in stability, and indicates a strong preference that the orbits be approximately coplanar. Multiple systems would be formed in successively higher levels of hierarchy and are discussed by Harrington (1977b).

Unlike triple stellar systems, which can form by gravitational capture, (*e.g.*, during the collision of two binary systems), such a formation mechanism would be difficult for asteroids because of the high encounter velocities relative to the orbital speeds (P. Hut, priv. comm.). The initial formation of triple/multiple systems were indicated, however, in the early numerical models of Durda (1996) and Doressoundiram *et al.* (1997) and are clearly produced by the next-generation models of Michel *et al.* (2001) and Durda *et al.* (2001). These SPH/N-body models of satellite formation show that in addition to producing binary systems with a single satellite in orbit about a primary asteroid, catastrophic disruption events can result (at least initially) in more complex, hierarchical systems with satellites of satellites. The gravitational reaccumulation of clumps of debris in the ejecta field around the largest remnant often leads to Shoemaker-Levy/9-like “strings-of-pearls”. Many of these reaccumulating rubble-pile fragments, some of which are gravitationally bound in initially stable orbits around the largest remnant, are themselves surrounded by swarms of smaller orbiting debris. The simulation timescales are too short, thus far, to directly examine the longer-term stability of these hierarchical satellite systems.

## 4 SUMMARY

The question posed in the title to the Weidenschilling *et al.* chapter in *Asteroids II*, “Do Asteroids have Satellites?”, has been answered. Now that we have many examples of binary systems

for study, representing diverse collisional and dynamical populations, we may be at the threshold of a revolution in asteroid science. In the *next* decade, we can expect to learn a great deal from the ever-increasing pace of discovery, involving several rapidly-improving, complementary techniques, and the concomitant numerical modeling and theoretical thinking about how these systems were formed, how they evolve, and what clues they hold to the history of the solar system. These binary systems will provide probes of asteroid interiors, and perhaps eventually allow definitive coupling of asteroid taxonomic type with our meteorite inventory. In fact, they may tell us about asteroid material for which it is unlikely we currently have representation among the meteorites, such as very low density carbonaceous material that may not survive passage through Earth's atmosphere, or primitive material of the outer Main-Belt, Trojan, or TNO regions. Research in this area will lead to spinoffs in related areas, including improvements in our understanding of the formation of the Earth/Moon or Pluto/Charon systems, better understanding of dynamics and collisional physics, and assist in the mitigation of the impact hazard that asteroids pose to Earth.

## REFERENCES:

1. André, C. Sur le système formé par la planète double (433) Eros. *Astron. Nachr.* **155**, 27–30 (1901).
2. Asphaug, E., Moore, J.M., Morrison, D., Benz, W., Nolan, M.C., & Sullivan, R.J. Mechanical and geological effects of impact cratering on Ida. *Icarus* **120**, 158–184 (1996).
3. Asphaug, E., Ostro, S.J., Hudson, R.S., Scheeres, D.J., & Benz, W. Disruption of kilometre-sized asteroids by energetic collisions. *Nature* **393**, 437–440 (1998).
4. Belton, M.J.S., Veverka, J., Thomas, P., Helfenstein, P., Simonelli, D., Chapman, C., Davies, M.E., Greeley, R., Greenberg, R., Head, J., Murchie, S., Klaasen, K., Johnson, T.V., McEwen, A., Morrison, D., Neukum, G., Fanale, F., Anger, C., Carr, M., & Pilcher, C. *Galileo* encounter with 951 Gaspra: first pictures of an asteroid. *Science* **257**, 1647–1652 (1992).
5. Belton, M. & Carlson, R. 1993 (243) 1. *IAU Circ.* **5948**, 2 (1994).
6. Belton, M.J.S., Chapman, C.R., Thomas, P.C., Davies, M.E., Greenberg, R., Klaasen, K., Byrnes, D., D'Amario, L., Synnott, S., Johnson, T.V., McEwen, A., Merline, W.J., Davis, D., Petit, J-M., Storrs, A., Veverka, J. & Zellner, B. Bulk density of asteroid 243 Ida from the orbit of its satellite Dactyl. *Nature* **374**, 785–788 (1995).
7. Belton, M.J.S., Mueller, B.E.A., D'Amario, L., Byrnes, D.V., Klaasen, K.P., Synnott, S., Breneman, H., Johnson, T.V., Thomas, P.C., Veverka, J., Harch, A.C., Davies, M.E., Merline, W.J., Chapman, C.R., Davis, D.R., Denk, T., Petit, J-M., Greenberg, R., Storrs, A.& Zellner, B. The discovery and orbit of 1993 (243) 1 Dactyl. *Icarus* **120**, 185–199 (1996).
8. Benner, L.A.M., Ostro, S.J., Giorgini, J.D., Jurgens, R.F., Margot, J.-L., & Nolan, M.C. 1999 KW<sub>4</sub>. *IAU Circ.* **7632**, 1 (2001a).
9. Benner, L.A.M., Nolan, M.C., Ostro, S.J., Giorgini, J.D., & Margot, J.-L. 1998 ST<sub>27</sub>. *IAU Circ.* **7730**, 2 (2001b).
10. Benz, W. & Asphaug, E. Simulations of brittle solids using smooth particle hydrodynamics. *Comput. Phys. Commun.* **87**, 253–265 (1995).
11. Binzel, R.P., Gaffey, M.J., Thomas, P.C., Zellner, B.H., Storrs A.D., & Wells, E.N. Geologic mapping of Vesta from 1994 Hubble Space Telescope images. *Icarus* **128**, 95–103 (1997).
12. Binzel, R.P. Collisional evolution in the Eros and Koronis asteroid families: observational and numerical results. *Icarus* **73**, 303–313 (1998).
13. Black, D.C. A simple criterion for determining the dynamical stability of three-body systems. *Astron. J.* **87**, 1333–1337 (1982).
14. Bottke, W.F., Nolan, M., & Greenberg, R. Velocity distributions among colliding asteroids. *Icarus* **107**, 255–268 (1994).
15. Bottke, Jr., W.F. & Melosh, H.J. The formation of asteroid satellites and doublet craters by planetary tidal forces. *Nature* **381**, 51–53 (1996a).

16. Bottke, Jr., W.F. & Melosh, H.J. The formation of binary asteroids and doublet craters. *Icarus* **124**, 372–391 (1996b).
17. Bottke, Jr., W.F., Richardson, D.C., Michel, P., & Love, S.G. 1620 Geographos and 433 Eros: Shaped by planetary tides? *Astron. J.* **117**, 1921–1928 (1999).
18. Britt, D.T. & Consolmagno, G.J. The porosity of dark meteorites and the structure of low-albedo asteroids. *Icarus* **146**, 213–219 (2000).
19. Britt, D.T. & Consolmagno, G.J. Modeling the structure of high porosity asteroids. *Icarus* **152**, 134–139 (2001).
20. Brown, M.E. & Margot, J.-L. S/2001 (87) 1. *IAU Circ.* **7588**, 1 (2001).
21. Brown, M.E. & Trujillo, C.A. (26308) 1998 SM<sub>165</sub>. *IAU Circ.* **7807**, 1 (2002).
22. Cellino, A., Pannunzio, R., Zappalà, V., Farinella, P., & Paolicchi, P. Do we observe light curves of binary asteroids? *Astron. Astrophys.* **144**, 355–362 (1985).
23. Chapman, C.R., Veverka, J., Thomas, P.C., Klaasen, K., Belton, M.J.S., Harch, A., McEwen, A., Johnson, T.V., Helfenstein, P., Davies M.E., Merline, W.J. & Denk, T. Discovery and physical properties of Dactyl, a satellite of asteroid 243 Ida. *Nature* **374**, 783–785 (1995).
24. Chapman, C.R. S-type asteroids, ordinary chondrites, and space weathering: the evidence from *Galileo*'s fly-bys of Gaspra and Ida. *Meteoritics & Planet. Sci.* **31**, 699–726 (1996).
25. Chapman, C.R., Ryan, E.V., Merline, W.J., Neukum, G., Wagner, R., Thomas, P.C., Veverka, J., & Sullivan, R.J. Cratering on Ida. *Icarus* **120**, 77–86 (1996).
26. Chauvineau, B. & Mignard, F. Dynamics binary asteroids II. Jovian perturbations. *Icarus* **87**, 377–390 (1990).
27. Chauvineau, B., Farinella, P., & Mignard, F. Planar orbits about a triaxial body: Applications to asteroidal satellites. *Icarus* **105**, 370–384 (1993).
28. Close, L.M., Merline, W.J., Tholen, D.J., Owen, T.C., Roddier, F., Dumas, C. Adaptive optics imaging of Pluto-Charon and the discovery of a moon around the asteroid 45 Eugenia: the potential of adaptive optics in planetary astronomy. *Proc. SPIE* **4007**, 787–795 (2000).
29. Davis, D.R., Chapman, C.R., Durda, D.D., Farinella, P., & Marzari, F. The formation and collisional/dynamical evolution of the Ida/Dactyl system as part of the Koronis family. *Icarus* **120**, 220–230 (1996).
30. Davis, R.G. High precision lightcurves for 762 Pulcova. *Minor Planet Bull.* **28**, 10–12 (2001).
31. Dell'Oro, A., Paolicchi, P., Cellino, A., & Zappalà, V. Collisional rates within newly formed asteroid families. *Icarus* **156**, 191–201 (2002).

32. Doressoundiram, A., Paolicchi, P., Verlicchi, A., & Cellino, A. The formation of binary asteroids as outcomes of catastrophic collisions. *Planet. Space. Sci.* **45**, 757–770 (1997).
33. Durda, D.D. The formation of asteroidal satellites in catastrophic collisions. *Icarus* **120**, 212–219 (1996).
34. Durda, D.D. & Geissler, P. The formation of asteroidal satellites in large cratering collisions. *Bull. Amer. Astron. Soc.* **28**, 1101 (1996).
35. Durda, D.D., Bottke, W.F., Asphaug, E., Richardson, D.C. The formation of asteroid satellites: Numerical simulations using SPH and N-body models. *Bull. Amer. Astron. Soc.* **33**, 5203 (2001).
36. Eggleton, P. & Kiseleva, L. An empirical condition for stability of hierarchical triple systems. *Astrophys. J.* **455**, 640–645 (1995).
37. Elliot, J.L., Kern, S.D., Osip, D.J., & Burles, S.M. 2001 QT<sub>297</sub>. *IAU Circ.* **7733**, 2 (2001).
38. Gehrels, T., Drummond, J.D. & Levenson, N.A. The absence of satellites of asteroids. *Icarus* **70**, 257–263 (1987).
39. Geissler, P., Petit, J.-M., Durda, D.D., Greenberg, R., Bottke, W., Nolan, M., & Moore, J. Erosion and ejecta reaccretion on 243 Ida and its moon. *Icarus* **120**, 140–157 (1996).
40. Goldreich, P. and S. Soter. Q in the solar system. *Icarus* **5**, 375–389 (1966).
41. Gradie, J. & Flynn, L. A search for satellites and dust belts around asteroids: negative results. *Proc. Lunar & Planetary Science Conf. XIX*, 405–406 (1988).
42. Graves, J.E., Northcott, M.J., Roddier, F.J., Roddier, C.A., & Close, L.M. First Light for Hokupa'a: 36-element curvature AO system at UH. *Proc. SPIE* **3353**, 34–43 (1998).
43. Hamilton, D.P. & Burns, J.A. Orbital stability zones about asteroids. *Icarus* **92**, 118–131 (1991).
44. Hansen, A.T. Arentoft, T., & Lang, K. The rotational period of 90 Antiope. *Minor Planet Bull.* **24**, 17 (1997).
45. Harrington, R.S. Planetary orbits in binary stars. *Astron. J.* **82**, 753–756 (1977a).
46. Harrington, R.S. A review of the dynamics of classical triple stars. *Rev. Mex. Astron. Astrofis.* **3**, 139–143 (1977b).
47. Harris, A.W. & Davies, J.K. Physical characteristics of near-Earth asteroids from thermal infrared spectrophotometry. *Icarus* **142**, 464–475 (1999).
48. Harris, A.W. On the slow rotation of asteroids. *Icarus* **156**, 184–190 (2002).
49. Hartmann, W.K. Diverse puzzling asteroids and a possible unified explanation. In *Asteroids* (T. Gehrels, Ed.), Univ. Arizona Press, Tucson, pp. 466–479 (1979).

50. Hudson, R.S. *Remote Sensing Reviews* **8**, 195–203 (1993).
51. Hudson, R.S. & Ostro, S.J. Shape of asteroid 4769 Castalia (1989 PB) from inversion of radar images. *Science* **263**, 940–943 (1994).
52. Kavelaars, J.J., Petit, J.-M., Gladman, B., & Holman, M. 2001 QW<sub>322</sub>. *IAU Circ.* **7749**, 1 (2001).
53. Kiseleva, L., Eggleton, P.P., & Orlov, V.V. Instability of close triple systems with coplanar initial doubly circular motion. *Mon. Not. R. Astron. Soc.* **270**, 936–946 (1994).
54. Leinhardt, Z.M., Richardson, D.C., & Quinn, T. Direct N-body simulations of rubble pile collisions. *Icarus* **146**, 133–151 (2000).
55. Leone, G., Farinella, P., Paolicchi, P., & Zappalà, V. Equilibrium models of binary asteroids. *Astron. Astrophys.* **140**, 265–272 (1984).
56. Love, S.G. & Ahrens, T.J. Origin of asteroid rotation rates in catastrophic impacts. *Nature* **386**, 154–156 (1997).
57. Margot, J.-L., Nolan, M.C., Benner, L.A.M., Ostro, S.J., Jurgens, R.F., Slade, M.A., Giorgini, J.D., & Campbell, D.B. Satellites of minor planets. *it IAU Circ.* **7503**, 2 (2000).
58. Margot, J.-L. & Brown, M.E. S/2001 (22) 1. *IAU Circ.* **7703**, 1 (2001).
59. Margot, J.-L., Nolan, M.C., Benner, L.A.M., Ostro, S.J., Jurgens, R.F., Giorgini, J.D., Slade, M.A., Howell, E.S., & Campbell, D.B. Radar discovery and characterization of binary near-Earth asteroids. *Proc. Lunar & Planetary Sci. Conf. XXXIII*, 1849 (2002a).
60. Margot, J.-L., Nolan, M.C., Benner, L.A.M., Ostro, S.J., Jurgens, R.F., Giorgini, J.D., Slade, M.A., & Campbell, D.B. Binary asteroids in the Near-Earth Object population. *Science* **296**, 1445–1448 (2002b).
61. Merline, W.J., Chapman, C.R., Robinson, M., Veverka, J., Harch, A., Bell III, J., Thomas, P., Clark, B.E., Joseph, J., Carcich, B., Murchie, S., Cheng, A., Izenberg, N., McFadden, L., & Malin, M. NEAR's encounter with 253 Mathilde: Search for satellites. *Proc. Lunar & Planetary Sci. Conf. XXIX*, 1954 (1998).
62. Merline, W.J., Chapman, C.R., Colwell, W.B., Veverka, J., Harch, A., Bell, M., Bell III, J., Thomas, P., Clark, B.E., Martin, P., Murchie, S., Cheng, A., Domingue, D., Izenberg, N., Robinson, M., McFadden, L., Wellnitz, D., Malin, M., Owen, W., & Miller, J. Search for satellites around asteroid 433 Eros from NEAR flyby imaging. *Proc. Lunar & Planetary Sci. Conf. XXX*, 2055 (1999a).
63. Merline, W.J., Close, L.M., Dumas, C., Chapman, C.R., Roddier, F., Ménard, F., Slater, D.C., Duvert, G., Shelton, C., Morgan, T., & Dunham, D.W. S/1998 (45) 1. *IAU Circ.* **7129**, 1 (1999b).

64. Merline, W.J., Close, L.M., Dumas, C., Chapman, C.R., Roddier, F., Ménard, F., Slater, D.C., Duvert, G., Shelton, C., Morgan, T. Discovery of a moon orbiting the asteroid 45 Eugenia. *Nature* **401**, 565–568 (1999c).
65. Merline, W.J., Close, L.M., Dumas, C., Shelton, J.C., Ménard, F., Chapman, C.R., Slater, D.C. Satellites of minor planets. *IAUC* **7503** (2000a).
66. Merline, W.J., Close, L.M., Dumas, C., Shelton, J.C., Ménard, F., Chapman, C.R., & Slater, D.C. Discovery of companions to asteroids 762 Pulcova and 90 Antiope by direct imaging. *Bull. Amer. Astron. Soc.* **32**, 1309 (2000b).
67. Merline, W.J., Ménard, F., Close, L., Dumas, C., Chapman, C.R., & Slater, D.C. S/2001 (22) 1. *IAU Circ.* **7703**, 1 (2001a).
68. Merline, W.J., Close, L.M., Siegler, N., Potter, D., Chapman, C.R., Dumas, C., Ménard, F., Slater, D.C., Baker, A.C., Edmunds, M.G., Mathlin, G., Guyon, O., & Roth, K. S/2001 (617) 1. *IAU Circ.* **7741**, 2 (2001b).
69. Merline, W.J., Tamblyn, P., Chapman, C.R., Colwell, W.B., Gor, V., Burl, M.C., Bierhaus, E.B., & Robinson, M.S. An automated search for moons during approach of the NEAR spacecraft to asteroid Eros. *Proc. 6th International Symposium on Artificial Intelligence, Robotics, and Automation in Space, 2001* (Montreal), CD-ROM, paper AM128 (2001c).
70. Merline, W.J., Close, L.M., Ménard, F., Dumas, C., Chapman, C.R., Slater, D.C. Search for asteroidal satellites. *Bull. Am. Astron. Soc.* **32**, 1017 (2001d).
71. Merline, W.J., Close, L.M., Siegler, N., Dumas, C., Chapman, C., Rigaut, F., Ménard, F., Owen, W.M., Slater, D.C. S/2002 (3749) 1. *IAU Circ.* **7827**, 2 (2002).
72. Michel, P., Benz, W., Tanga, P., Richardson, D.C. Collisions and gravitational re-accumulation: Forming asteroid families and satellites. *Science* **294**, 1696–1700 (2001).
73. Miller, M.C. & Hamilton, D.P. Four-body effects in globular cluster black hole coalescence. *Astron. J.*, in press (2002).
74. Mottola, S., De Angelis, G., Di Martino, M., Erikson, A., Hahn, G., and Neukum, G. The near-Earth objects follow-up program: First results. *Icarus* **117**, 62–70 (1995).
75. Mottola, S., Hahn, G., Pravec, P., and Šarounová, L. S/1997 (3671) 1. *IAU Circ.* **6680**, 2 (1997).
76. Mottola, S. and Lahulla, F. Mutual eclipse events in asteroidal binary system 1996 FG<sub>3</sub>: Observations and a numerical model. *Icarus* **146**, 556–567 (2000).
77. Nolan, M.C., Margot, J.-L., Howell, E.S., Benner, L.A.M., Ostro, S.J., Jurgens, R.F., Giorgini, J.D., & Campbell, D.B. 2000 UG<sub>11</sub>. *IAU Circ.* **7518**, 2 (2000).
78. Nolan, M.C., Howell, E.S., Magri, C., Beeney, B., Campbell, D.B., Benner, L.A.M., Ostro, S.J., Giorgini, J.D., Margot, J.-L. 2002 BM<sub>26</sub>. *IAU Circ.* **7824**, 1 (2002).

79. Noll, K., Stephens, D., Grundy, W., Spencer, J., Millis, R., Buie, M., Cruikshank, D., Tegler, S., Romanishin, W. 1997 CQ<sub>29</sub>. *IAU Circ.* **7824**, 2 (2002a).
80. Noll, K., Stephens, D., Grundy, W., Spencer, J., Millis, R., Buie, M., Cruikshank, D., Tegler, S., Romanishin, W. 2000 CF<sub>105</sub>. *IAU Circ.* **7857**, 1 (2002b).
81. Ostro, S.J., Chandler, J.F., Hine, A.A., Rosema, K.D., Shapiro, I.I., & Yeomans, D.K. Radar images of asteroid 1989 PB. *Science* **248**, 1523–1528 (1990).
82. Ostro, S.J., Hudson, R.S., Nolan, M.C., Margot, J.-L., Scheeres, D.J., Campbell, D.B., Margi, C., Giorgini, J.D., & Yeomans, D.K. Radar observations of asteroid 216 Kleopatra. *Science* **288**, 836–839 (2000a).
83. Ostro, S.J., Margot, J.-L., Nolan, M.C., Benner, L.A.M., Jurgens, R.F., Giorgini, J.D. 2000 DP<sub>107</sub>. *IAU Circ.* **7496**, 2 (2000b).
84. Petit, J.-M., Durda, D.D., Greenberg, R., Hurford, T.A., Geissler, P.E. The long-term stability of Dactyl's orbit. *Icarus* **130**, 177–197 (1997).
85. Pravec, P. Rotation studies and orbital distribution of near-Earth asteroids. PhD Thesis. Charles Univ. Prague (1995).
86. Pravec, P., Wolf, M., Varady, M., and Bárta, P. CCD photometry of 6 near-Earth asteroids. *Earth Moon Planets* **71**, 177–187 (1995).
87. Pravec, P. & Hahn, G. Two-period lightcurve of 1994 AW<sub>1</sub>: Indication of a binary asteroid? *Icarus* **127**, 431–440 (1997).
88. Pravec, P., Wolf, M., Šarounová, L. Occultation/eclipse events in binary asteroid 1991 VH. *Icarus* **133**, 79–88 (1998).
89. Pravec, P., Šarounová, L., & Wolf, M. 1996 FG<sub>3</sub>. *IAU Circ.* **7074**, 2 (1998).
90. Pravec, P., Wolf, M., Šarounová, L. How many binaries are there among near-Earth asteroids? In *Evolution and Source Regions of Asteroids and Comets, Proc. IAU Coll. 173*, (J. Svoreň, E. M. Pittich, and H. Rickman, eds.), pp. 159–162. Astron. Inst. Slovak Acad. Sci., Tatranská Lomnica (1999).
91. Pravec, P. & Harris, A.W. Fast and slow rotation of asteroids. *Icarus* **148**, 12–20 (2000).
92. Pravec, P., Šarounová, L., Rabinowitz, D.L., Hicks, M.D., Wolf, M., Krugly, Y.N., Velichko, F.P., Shevchenko, V.G., Chiorny, V.G., Gaftonyuk N.M., & Genevier, G. Two-period lightcurves of 1996 FG<sub>3</sub>, 1998 PG, and (5407) 1992 AX: One probable and two possible binary asteroids. *Icarus* **146**, 190–203 (2000a).
93. Pravec, P., Kusnirak, P., Hicks, M., Holliday, B., & Warner, B. 2000 DP<sub>107</sub>. *IAU Circ.* **7504**, 2 (2000b).
94. Pravec, P. & Šarounová, L. 1999 KW<sub>4</sub>. *IAU Circ.* **7633**, 2 (2001).

95. Pravec, P., Kusnirak, P., & Warner, B. 2001 SL<sub>9</sub>. *IAU Circ.* **7742**, 3 (2001).
96. Pravec, P., Šarounová, L., Hicks, M.D., Rabinowitz, D.L., Wolf, M., Scheirich, P., Krugly, Y.N. Two periods of 1999 HF<sub>1</sub> — another binary NEA candidate. *Icarus*, in press (2002a).
97. Reitsema, H.J. The reliability of minor planet satellite observations. *Science* **205**, 185–186 (1979).
98. Richardson, D.C., Bottke, W., & Love, S.G. Tidal distortion and disruption of Earth-crossing asteroids. *Icarus* **134**, 47–76 (1998).
99. Rigaut, F., Salmon, D., Arsenault, R., Thomas, J., Lai, O., Rouan, D., Véran, J.P., Gigan, P., Crampton, D., Fletcher, J.M., Stilburn, J., Boyer, C., & Jagourel, P. Performance of the Canada-France-Hawaii Telescope adaptive optics bonnette. *Pub. Astron. Soc. Pacific* **110**, 152–164 (1998).
100. Roberts, Jr., L.C., McAlister, H.A., & Hartkopf, W.I. A speckle interferometric survey for asteroid duplicity. *Astron. J.* **110**, 2463–2468 (1995).
101. Roddier F., Curvature sensing and compensation: a new concept in adaptive optics. *Applied Optics* **27**, 1223–1225 (1988).
102. Roddier F., Northcott, M. and Graves J.E., A simple low-order adaptive optics system for near infrared applications. *Pub. Astron. Soc. Pac.* **103**, 131–149 (1991).
103. Scheeres, D.J. Dynamics about uniformly rotating tri-axial ellipsoids. *Icarus* **110**, 225–238 (1994).
104. Showalter, M.R., Ostro, S.J., Shapiro, I.I., & Campbell, D.B. Upper limit on the radar cross section of a Pallas satellite. *Bull. Amer. Astron. Soc.* **14**, 725 (1982).
105. Storrs, A., Wells, E., Stern, A., & Zellner, B. Surface heterogeneity of asteroids: HST WFPC2 images 1996-1997. *Bull. Amer. Astron. Soc.* **30**, 1026 (1998).
106. Storrs, A., Weiss, B., Zellner, B., Burleson, W., Sichtiu, R., Wells, E., Kowal, C., & Tholen, D. Imaging observations of asteroids with Hubble Space Telescope. *Icarus* **137**, 260–268 (1999a).
107. Storrs, A.D., Wells, E.N., Zellner, B.H., Stern, A., & Durda, D. Imaging observations of asteroids with HST. *Bull. Amer. Astron. Soc.* **31**, 1089 (1999b).
108. Storrs, A., Vilas, F., Landis, R., Wells, E., Woods, C., Zellner, B., & Gaffey, M. S/2001 (107) 1. *IAU Circ.* **7599**, 1 (2001).
109. Tanga, P., Hestroffer, D., Berthier, J., Cellino, A., Lattanzi, M.G., Di Martino, M., & Zapalà, V. HST/FGS observations of asteroid (216) Kleopatra. *Icarus* **153**, 451–454 (2001).
110. Toth, I. On the detectability of satellites of small bodies orbiting the Sun in the inner region of the Edgeworth-Kuiper Belt. *Icarus* **141**, 420–425 (1999).

111. Trujillo, C.A. & Brown, M.E. 1999 TC<sub>36</sub>. *IAU Circ.* **7787**, 1 (2002).
112. Van Flandern, T.C., Tedesco, E.F. & Binzel, R.P. Satellites of asteroids. In *Asteroids* (ed. Gehrels, T.) pp. 443–465 (Univ. of Arizona Press) (1979).
113. Veillet, C., Doressoundiram, A., Shapiro, J., Kavelaars, J.J., Morbidelli, A. S/2000 (1998 WW<sub>31</sub>) 1. *IAU Circ.* **7610**, 1 (2001).
114. Veillet, C., Parker, J.W., Griffin, I., Marsden, B., Doressoundiram, A., Buie, M., Tholen, D.J., Connelley, M., & Holman, M.J. The binary Kuiper-belt object 1998 WW<sub>31</sub>. *Nature* **416**, 711–713 (2002).
115. Veverka, J., Helfenstein, P., Lee, P., Thomas, P., McEwen, A., Belton, M., Klaasen, K., Johnson, T.V., Granahan, J., Fanale, F., Geissler, P., & Head III, J.W. Ida and Dactyl: Spectral reflectance and color variations. *Icarus* **120**, 66–76 (1996a).
116. Veverka, J., Thomas, P.C., Helfenstein, P., Lee, P., Harch, A., Calvo, S., Chapman, C., Belton, M.J.S., Klaasen, K., Johnson, T.V., & Davies, M. Dactyl: *Galileo* observations of Ida's satellite. *Icarus* **120**, 200–211 (1996).
117. Veverka, J., Thomas, P., Harch, A., Clark, B., Bell III, J.F., Carcich, B., & Joseph, J., Murchie, S., Izenberg, N., Chapman, C., Merline, W., Malin, M., McFadden, L., & Robinson, M. *NEAR* encounter with asteroid 253 Mathilde: Overview. *Icarus* **140**, 3–16 (1999a).
118. Veverka, J., Thomas, P.C., Bell III, J.F., Bell, M., Carcich, B., Clark, B., Harch, A., Joseph, J., Martin, P., Robinson, M., Murchie, S., Izenberg, N., Hawkins, E., Warren, J., Farquhar, R., Cheng, A., Dunham, D., Chapman, C., Merline, W.J., McFadden, L., Wellnitz, D., Malin, M., Owen Jr., W.M., Miller, J.K., Williams, B.G., & Yeomans, D.K. Imaging of asteroid 433 Eros during *NEAR*'s flyby reconnaissance. *Science* **285**, 562–564 (1999b).
119. Veverka, J., Robinson, M., Thomas, P., Murchie, S., Bell III, J.F., Izenberg, N., Chapman, C., Harch, A., Bell, M., Carcich, B., Cheng, A., Clark, B., Domingue, D., Dunham, D., Farquhar, R., Gaffey, M.J., Hawkins, E., Joseph, J., Kirk, R., Li, H., Lucey, P., Malin, M., Martin, P., McFadden, L., Merline, W.J., Miller, J.K., Owen, Jr., W.M., Peterson, C., Prokter, L., Warren, J., Wellnitz, D., Williams, B.G., & Yeomans, D.K. *NEAR* at Eros: imaging and spectral results. *Science* **289**, 2088–2097 (2000).
120. Weidenschilling, S.J., Paolicchi, P. & Zappalà, V. Do asteroids have satellites? In *Asteroids II* (eds. Binzel, R., Gehrels, T. & Matthews, M.) pp. 643–658 (Univ. of Arizona Press) (1989).
121. Weidenschilling, S.J., Marzari, F., Davis, D.R., & Neese, C. Origin of the double asteroid 90 Antiope: A continuing puzzle. *Proc. Lunar & Planetary Sci. Conf. XXXII*, 1890 (2001).
122. Wizinowich, P.L., Acton, D.S., Lai, O., Gathright, J., Lupton, W., Stomski, P.J. Performance of the W.M. Keck Observatory natural guide star adaptive optic facility: The first year at the telescope. *Proc. SPIE* **4007**, 2–13 (2000).

123. Zellner, B., Wells, E.N., Chapman, C.R., & Cruikshank, D.P. Asteroid observations with the Hubble Space Telescope and the Space Infrared Telescope Facility. In *Asteroids II* (Binzel, Gehrels, and Matthews, eds.) pp. 949–969 (1989).

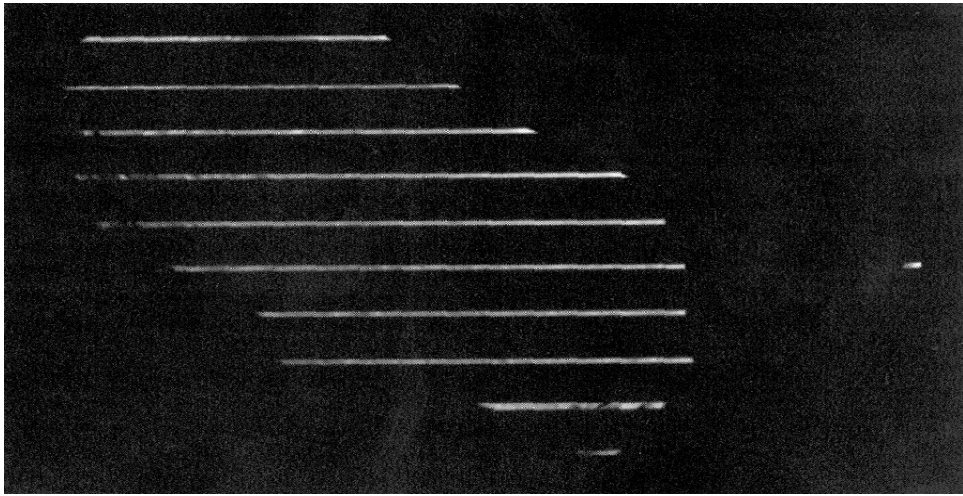


Figure 1: This is the discovery image for Dactyl, the first known asteroid satellite (Belton *et al.* 1996). It was taken by the *Galileo* spacecraft on 1993 Aug 29 from a range of 10,719 km. The picture has a resolution of about 100 m/pix. Because of limited downlink, not all images could be returned. Instead, this technique of playing back image strips was used to find the relevant images or portions of images that contained Ida. The resulting “jailbar” image here fortuitously provided the first clue of an extended object, with the expected photometric profile, off the bright limb of Ida.



Figure 2: This full image of Ida and Dactyl, taken from approximately the same range and with the same resolution listed in Figure 1. The picture is in a green filter. Ida is about 56 km long and Dactyl is roughly spherical with a diameter of about 1.4 km. At this time Dactyl is in the foreground, about 85 km ( $5.5 R_{Ida}$ ) from Ida's center, and moving at about  $6 \text{ m s}^{-1}$ . The orbit is prograde with respect to Ida's spin, which itself is retrograde with respect to the ecliptic.



Figure 3: Highest resolution picture of Dactyl, at 39 m/pix, showing shape and surface geology. The topography is dominated by impact craters, without prominent grooves or ridges.

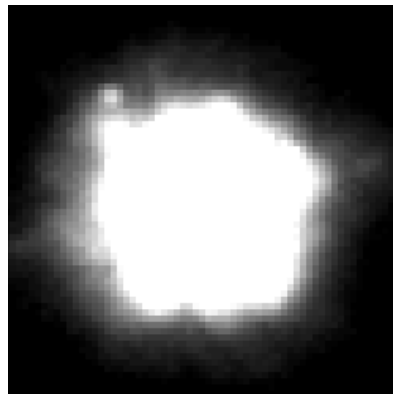


Figure 4: This is the discovery image of Petit Prince, moon of (45) Eugenia, taken at the Canada-France-Hawaii Telescope on 1998 Nov 1, using the PUEO adaptive optics system (Merline *et al.* 1999b). It is the first asteroid moon to be imaged from Earth. The image is an average of 16 images of exposure 15 s. It is taken in H-band ( $1.65 \mu\text{m}$ ) and has a plate scale of 0.035 arcsec/pixel. The separation of the moon is about 0.75 arcsec from Eugenia and has a brightness ratio of about 7 magnitudes.

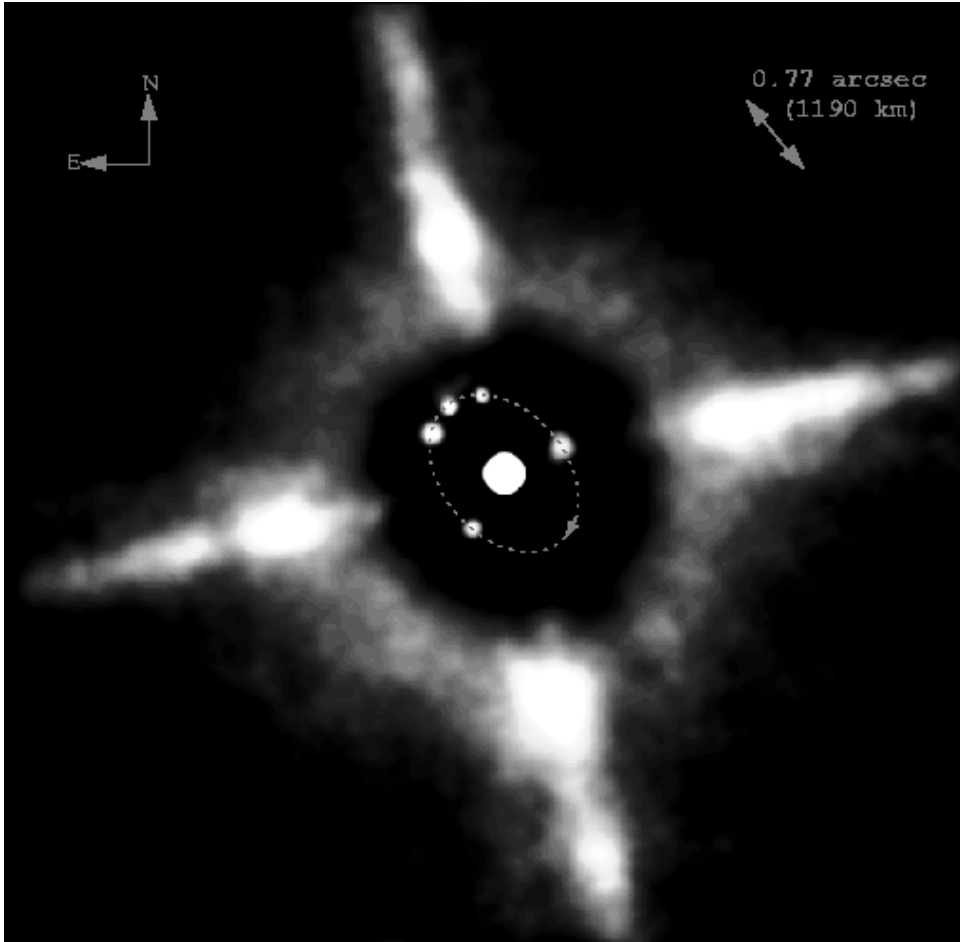
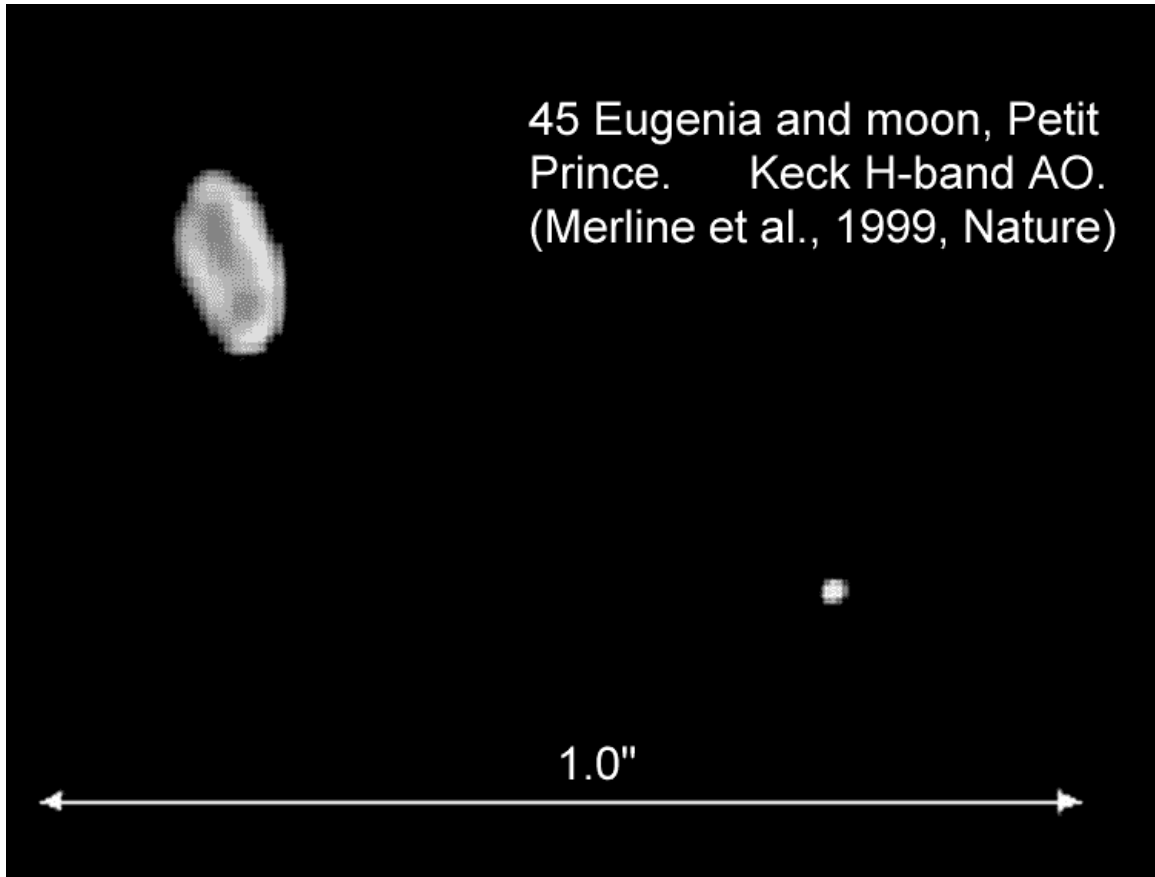


Figure 5: This infrared image is a composite of 5 epochs of Eugenia’s moon. The moon has a period is 4.7 days, with a nearly circular orbit is about 1190 km (0.77 arcsec). The orbit is tilted about 46 degrees with respect to our line-of-sight. The normal 2-fold degeneracy in pole position (*i.e.*,true sense of the moon’s orbit) was resolved by observing the system later, when positional differences between the two solutions became apparent. Eugenia is about 215 km in diameter and the moon’s diameter is about 13 km. The large “cross” is a common artifact of diffraction from the secondary-mirror support structure. The images are deconvolved and the brightness of Eugenia has been suppressed to enhance sharpness and clarity.



45 Eugenia and moon, Petit  
Prince. Keck H-band AO.  
(Merline et al., 1999, Nature)

Figure 6: This deconvolved Keck image in 2000 Feb shows Petit Prince and a resolved image of the disk of Eugenia (after Close *et al.* 2000). The pair is well-separated, enough to get accurate colors or spectra. The unusual elongation of Eugenia's shape was inferred previously from lightcurve amplitudes. Because the lack of detailed fidelity in flux preservation under deconvolution, the brightness variations across the disk are not real. The brightness of the satellite (which is not resolved) has been scaled to appear to have roughly the same “surface brightness” as the primary. The flux ratio of the two objects is about 285.

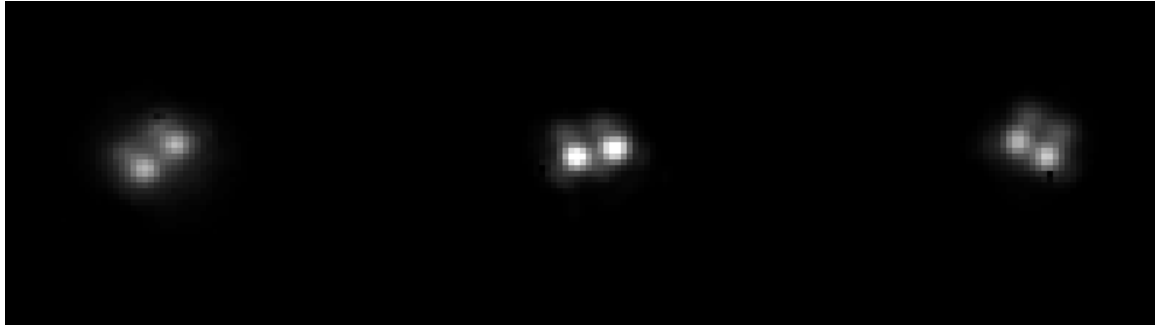


Figure 7: Double asteroid (90) Antiope as it rotates with a 16.5 h period, soon after its discovery at Keck in 2000 August (Merline *et al.* 2000a,b). Once thought to be an object about 125 km across, the C-type asteroid Antiope actually has two components, each about 85 km in diameter. The separation is about 170 km.

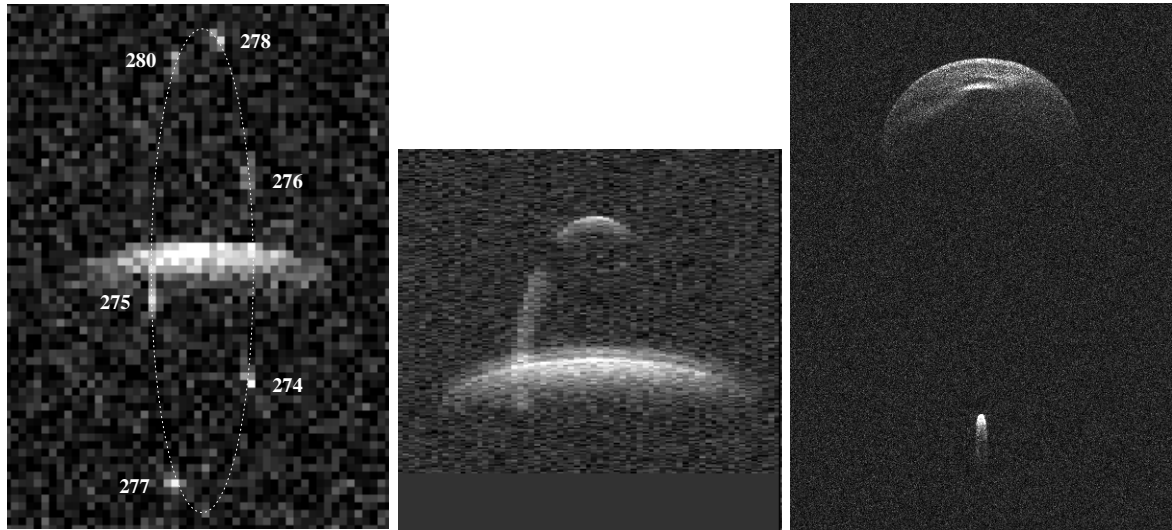


Figure 8: (a) Arecibo delay-Doppler images of binary asteroid 2000 DP<sub>107</sub> (Margot *et al.* 2002b) obtained on 2000 DOY 274–280. A dashed line shows the approximate trajectory of the companion on consecutive days. (b) Goldstone radar echoes of 1999 KW<sub>4</sub> (Ostro *et al.*, JPL press release) accumulated over several-hours during its May 2001 close approach to Earth. (c) Radar image of 1999 KW<sub>4</sub> obtained at Arecibo on 2001 May 27 with 7.5 m range resolution. Range from the observer increases down and Doppler frequency increases to the right. Dimensions in the cross-range dimension are affected by the primary and secondary spin rates.

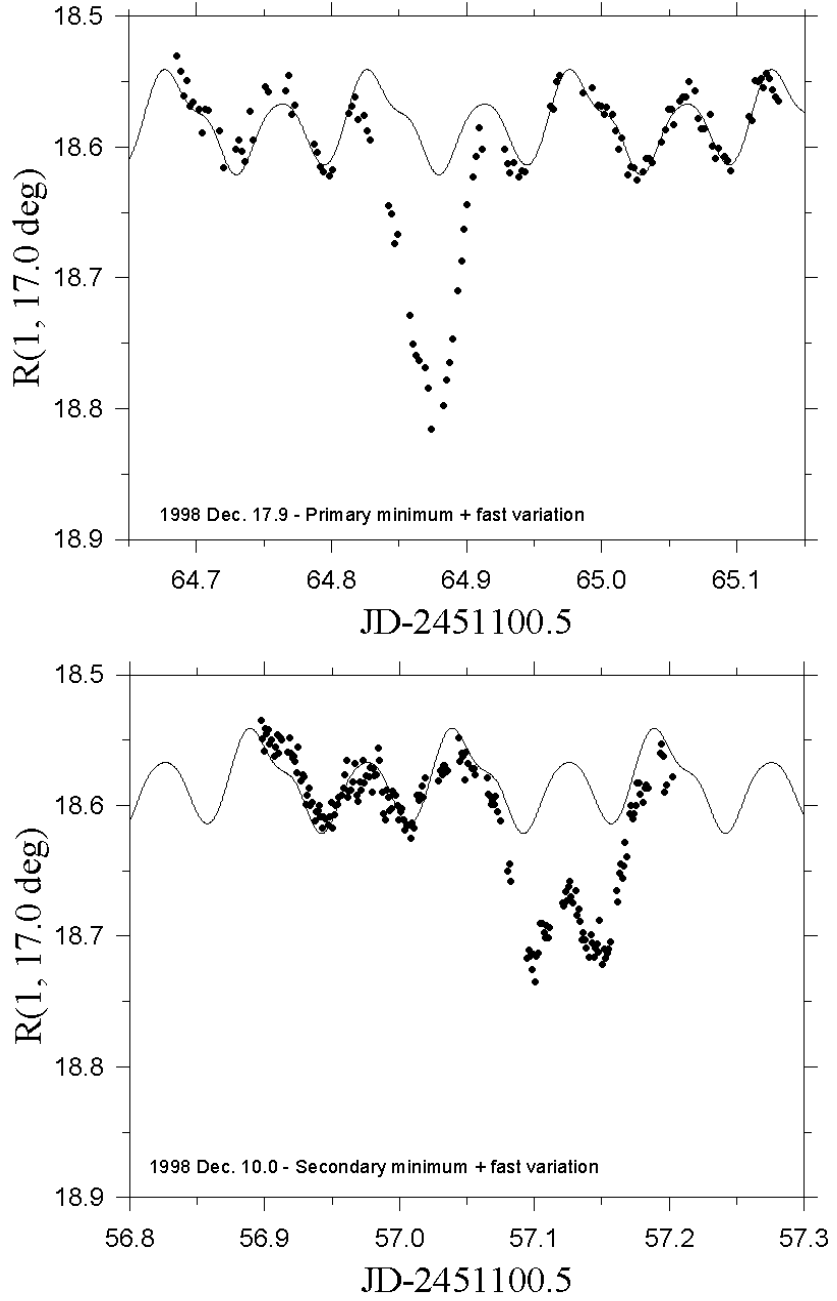


Figure 9: Observed lightcurves of 1996 FG<sub>3</sub> show the fast-variation, small-amplitude component, caused by the rotation of the primary, with superposed sudden sharp attenuations caused by the eclipse/occultation of the primary by the secondary. The top panel shows the primary minimum, while the bottom panel shows the secondary minimum. The primary rotation component can be seen also during the attenuations. (From Pravec *et al.* 2000a).

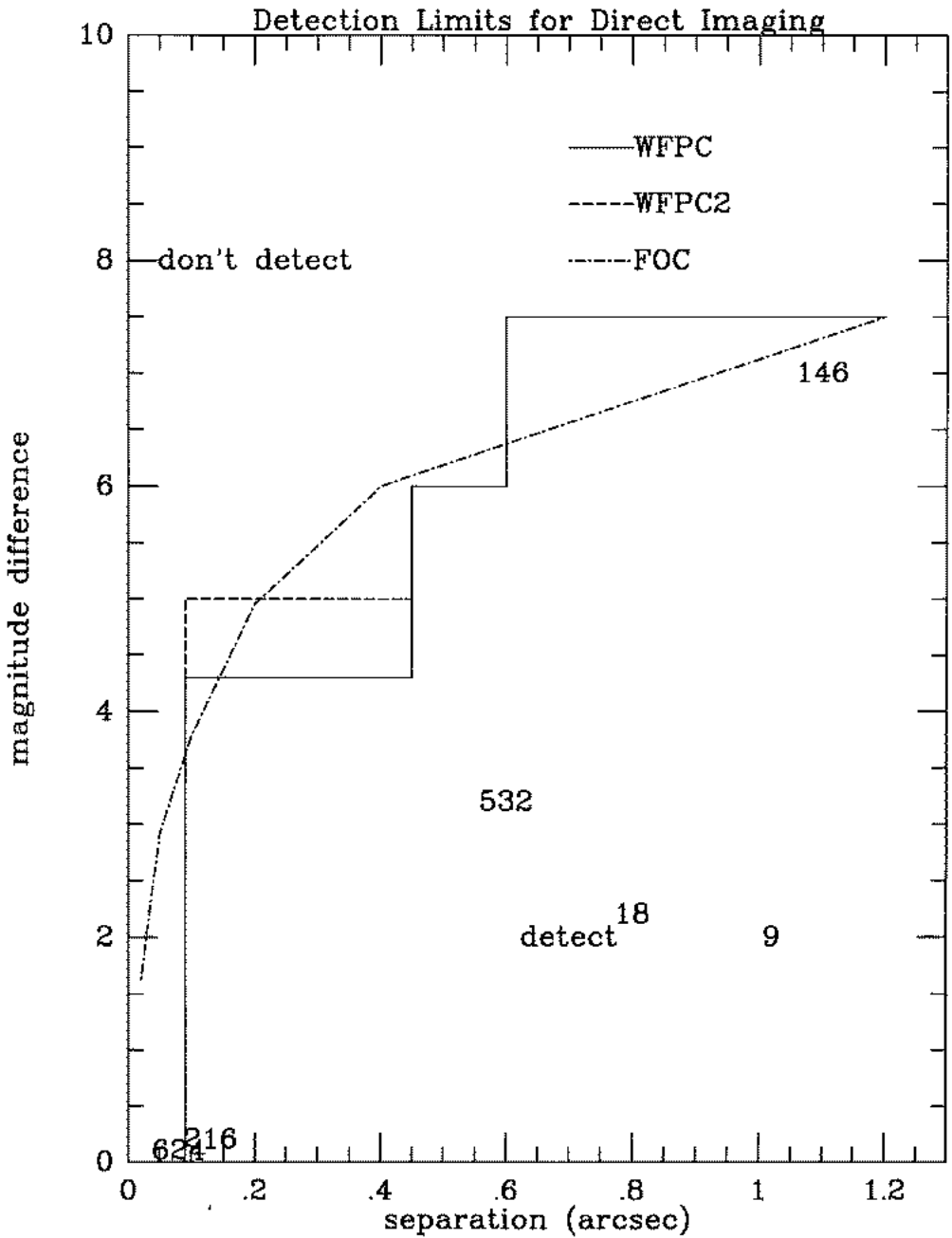


Figure 10: Brightness difference (in magnitudes) between a primary asteroid and a possible companion, as a function of projected distance from the primary asteroid, for well-exposed HST images (after Storrs *et al.* 1999a). The region below the curves is where companions could be detected. Also shown are the locations of putative binaries (given by asteroid number) that had been previously suspected from occultation or other data.

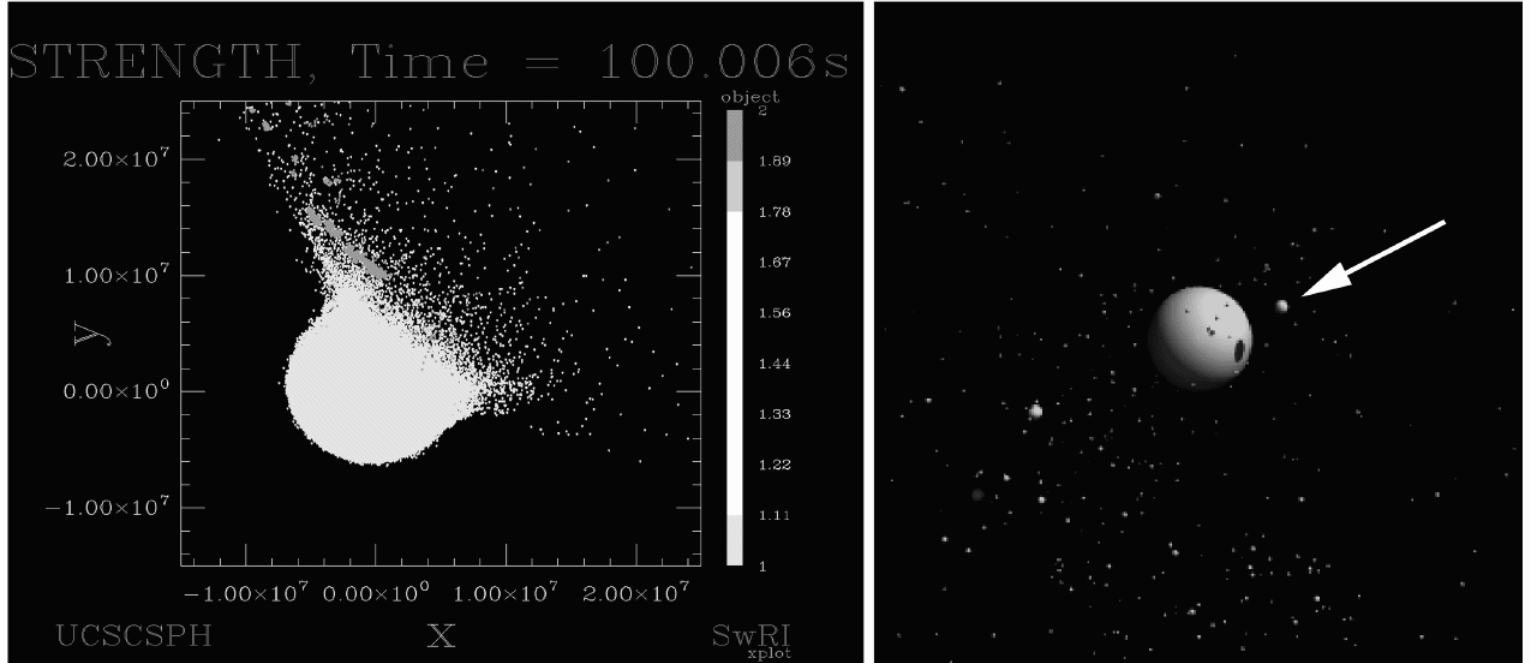


Figure 11: The “next generation” of numerical models of asteroid satellite formation substantially improve upon past models by (left) conducting detailed 3-dimensional smooth-particle hydrodynamics (SPH) models of collisions between asteroids and then (right) following the subsequent dynamics of ejected debris and formation of orbiting satellites (arrow) through fast, state-of-the-art N-body simulations. Shown here is a collision of a 20 km impactor into a 100 km solid basaltic target, as simulated by Durda *et al.* (2001). The satellite of size about 4 km is captured into an elliptical orbit with a separation of about  $6 R_{\text{primary}}$ . The final primary diameter is about 75 km.